Structure factor of thin films near continuous phase transitions

R. Klimpel and S. Dietrich
Fachbereich Physik, Bergische Universität Wuppertal, D-42097 Wuppertal, Federal Republic of Germany
(Received 23 April 1999)

The two-point correlation function in thin films is studied near the critical point of the corresponding bulk system. Based on field-theoretic renormalization-group theory, the dependences of this correlation function on the lateral momentum, the two distances normal to the free surfaces, the temperature, and the film thickness are determined. The corresponding scattering cross section of x rays and neutrons under grazing incidence is calculated. This reveals the various singularities of the two-point correlation function.
[S0163-1829(99)03732-7]

I. INTRODUCTION

Structural properties of condensed matter depend sensitively on the space dimension d. Thin films offer the opportunity to reveal this dependence. By varying the film thickness L, one can interpolate smoothly between $d=2$ and 3. For crystalline materials this variation can be accomplished with atomic resolution by using molecular-beam epitaxy.[1] As an alternative, which is also applicable for fluids, thin films can be built up via wetting phenomena where the film thickness is controlled by temperature or chemical potentials.[2] Once such films are prepared, the dependence of their structural properties on the space dimension can be studied particularly clearly close to phase transitions. For first-order phase transitions the main influence of a variation of the film thickness is to shift the phase boundaries in the phase diagram (see, e.g., capillary condensation[3] or the shift of the melting curve[4]) without much changing the *local* properties of condensed matter. In rare cases, however, even the *character* of the phase transition can change as function of L; see, e.g., the possibility of continuous melting in $d=2$ (Refs. 5) as opposed to $d=3$, or the crossover from a first-order phase transition in $d=3$ to a second-order phase transition in $d=2$ at a certain thickness of a slab of the three-states Potts model.[6]

In the case of *first-order* phase transitions, the robustness of the local structural properties with respect to changes of the film thickness is due to the smallness of the correlation lengths which characterize these systems and—putting aside possible wetting phenomena—thus severely limit the propagation of the structural changes, which necessarily occur near the confining surfaces of the film, into the interior of the films. In contrast, *second-order* phase transitions are characterized by diverging correlation lengths which affect not only the location of phase boundaries but in addition lead to pronounced changes in the local properties even deep in the interior of the films if the critical point is approached. These effects are thus not only particularly suitable to shed light on the aforementioned dependence of the structural properties on space dimension, but they offer an additional advantage: the divergence of the correlation length as a function of temperature upon approaching the critical point leads to a *universal* behavior, which makes a *quantitative* comparison between theoretical predictions and experiments much easier as compared with systems exhibiting first-order phase transitions, which are characterized by several competing length scales of comparable, atomic size which are difficult to determine accurately and to vary systematically and independently.

A sizable body of theoretical research has emerged describing continuous phase transitions in thin films (see, e.g., Refs. 7–17). Initiated by the theory of finite-size scaling (see, e.g., Refs. 18–23), *inter alia* the shift $T_c(L)$ of the critical temperature with respect to its bulk value $T_c \equiv T_c(L=\infty)$,[24–26] the magnetization[27,28] as well as the free energy, the Casimir force, and the specific heat[29–35] have been analyzed. Here we emphasize that in order to observe universal film behavior, the thicknesses L of the films still have to be large on an atomic scale. This is assumed to be the case throughout our analysis. The analytic description of the dimensional crossover between $d=3$ critical behavior near T_c and the $d=2$ critical behavior near $T_c(L)$ still poses a challenge[36,37] which has not yet been overcome with satisfactory quantitative accuracy. Numerous experiments (see, e.g., Refs. 38–43) and simulations (see, e.g., Refs. 44–46) have been carried out to test these theoretical predictions. They lend support to the finite-size scaling theory, but still pose a puzzle as a far as a detailed quantitative agreement is concerned.

The vast majority of these studies has been devoted to integral or excess quantities without spatial resolution. However, studies of *local* critical properties, such as of one- and two-point correlation functions, near a *single* surface have revealed a wealth of universal phenomena featuring numerous surface critical exponents and interesting crossover phenomena—on the scale of the bulk correlation length ξ—between surface and bulk critical behavior;[47,48] the integral and excess quantities offer either no or only very limited access to these local properties.

The successful development of surface-specific x-ray and neutron-scattering techniques based on exploiting total external reflection at grazing incidence has proven to be very fruitful, *inter alia*, for facilitating a quantitative comparison between experiments and theoretical predictions of the local critical behavior near interfaces.[49,50] These scattering techniques allow one to determine order-parameter profiles normal to the surface, and a depth-resolved lateral two-point correlation function. In the present context such experiments

have been carried out successfully for the binary alloy Fe_3Al,[51–53] and, by using truncation rod scattering, for FeCo,[54] which exhibit continuous order-disorder transitions in the bulk. In the case of Fe_3Al the cusplike surface singularities of the momentum and temperature dependence of the two-point correlation function turned out to be in excellent agreement with the theoretical predictions.[55,56] The fact that, due to the occurrence of surface segregation, suitable choices for the crystallographic orientation of the surface allows one to switch between the different surface universality classes corresponding to free boundary conditions and boundary conditions with surface fields, respectively, of the same bulk sample,[57,58] offers wide ranges of interesting comparative studies.

In view of these developments, and in view of the increasing availability of powerful synchrotron and neutron sources, it appears promising to extend these studies of local critical properties to thin films. There are several predictions concerning the behavior of one-point correlation functions in thin films such as order-parameter profiles[27,28,35] and energy-density profiles.[59] However, on the level of the two-point correlation function, so far only very little is known. This function depends on the lateral distance $\mathbf{x}_\parallel = \mathbf{x}_\parallel^{(2)} - \mathbf{x}_\parallel^{(1)}$ between the two points $\mathbf{x}_1 = (\mathbf{x}_\parallel^{(1)}, z_1)$ and $\mathbf{x}_2 = (\mathbf{x}_\parallel^{(2)}, z_2)$ (or equivalently the lateral momentum $\mathbf{p}$ corresponding to the $d-1$ translationally invariant directions), the coordinates z_1 and z_2 perpendicular to the parallel surfaces of the film, the film thickness L, and temperature $t = (T - T_c)/T_c$ (or equivalently the bulk correlation length $\xi = \xi_0 t^{-\nu}$). Since a full sweep of this large parameter space is practically not possible for computer simulations, we have applied field-theoretic techniques which provide analytic access to the full parameter space. This approach encompasses nonperturbative features such as scaling properties and short-distance expansions, as well as an explicit and systematic perturbative result to first order in $\epsilon = 4 - d$. The latter serves to corroborate the nonperturbative results and to provide numerical results which are not accessible by general arguments. These explicit calculations are carried out for the fixed point of the so-called ordinary transition for both confining surfaces in the classification scheme of surface critical phenomena[48] corresponding to free boundary conditions on both sides. This is applicable to thin antiferromagnetic films near their Néel temperature, to ferromagnetic films near their Curie temperature in the absence of external bulk and surface fields, and to thin films of binary alloys near their continuous order-disorder transitions. Among the numerous order-disorder phase transitions in binary alloys, only a few are of second order including, Fe_3Al,[60–62] FeCo,[63] CuZn,[64] and FeAl.[61] Both the $B2$–DO_3 transition in Fe_3Al and the $A2$–$B2$ transitions in FeCo, CuZn, and FeAl belong to the Ising universality class.[65] For the $A2$–$B2$ transitions it is predicted theoretically that the (110) surface belongs to the surface universality class of the ordinary transition, whereas the (100) surface exhibits the so-called normal transition associated with the presence of an effective surface field.[57,58] Indeed, truncation rod scattering at the FeCo (100) surface has provided clear evidence for the presence of an effective surface field[54] above T_c, although the expected associated crossover from ordinary to normal critical behavior[66] could not yet been resolved experimentally in an unequivocal way. The results of the diffuse scattering of x rays under grazing incidence from the $(1\bar{1}0)$ surface [equivalent to the (110) surface] of Fe_3Al (Ref. 51) are in excellent agreement with the theoretical predictions[55,56] for the ordinary transition. But even for Fe_3Al $(1\bar{1}0)$ a residual order parameter above T_c has been reported.[51,52] Thus it still remains to be seen theoretically whether for the $B2$–DO_3 transition in Fe_3Al, in contrast to the $A2$–$B2$ transition in FeCo, the $(1\bar{1}0)$ surface can support a weak effective surface field. In view of this state of affairs our present result are expected to be closely applicable to thin films of Fe_3Al, FeCo, CuZn, and FeAl bounded by (110) surfaces on both sides. Among them Fe_3Al and FeCo appear to be the most promising candidates because the others exhibit strong surface segregation. For an assessment of the possibilities to probe critical magnetic surface transitions by grazing incidence of neutrons see Ref. 67.

In view of the aforementioned difficulties concerning the analytic description of the dimensional crossover we confine our analysis to the temperature range $T \geqslant T_c$. We note that elements of the perturbation theory for thin critical films can be found in Ref. 68. However, we had to carry out our own approach because the representation given in Ref. 68 is not suited for making predictions for the scattering experiments, and because Ref. 68 contains errors. Finally we note that experience tells us that calculations carried out for the spherical model, as have been done for the present system,[69] lack the quantitative reliability needed for comparison with experiments and simulations.

In order to encourage future scattering experiments for critical thin films and to facilitate an explicit quantitative comparison of such data with the present theoretical predictions, we have calculated the singular contributions to the scattering cross section for x-ray and neutron scattering under the condition of grazing incidence based on our results for the critical two-point correlation function in thin films. This allows us to describe the conditions under which the various singularities of the two-point correlation function become visible in scattering data.

This introduction is followed by three sections, a summary, and four Appendixes. In Sec. II we introduce the field-theoretical model. The two-point correlation function is discussed in Sec. III, and in Sec. IV we investigate the scattering cross section. Relations between bulk and film amplitudes are derived in Appendix A, explicit one-loop results are presented in Appendix B, and Appendixes C and D contain details required for the calculation of the scattering cross section.

II. FIELD-THEORETICAL MODEL

The leading critical behavior in a film follows from the statistical weight $\exp(-\mathcal{H}\{\Phi\})$ for the configuration $\Phi(\mathbf{x}) = (\phi_a(\mathbf{x}), a = 1, \ldots, n)$ of an n-component field, which is

proportional to the order parameter, where[48,30,32]

$$\mathcal{H}\{\Phi(\mathbf{x})\}=\int d^{d-1}x_{\parallel}\int_0^L dz\left(\frac{1}{2}(\nabla\Phi)^2+\frac{\tau}{2}\Phi^2+\frac{g}{4!}(\Phi^2)^2-\mathbf{h}\cdot\Phi\right)+\int d^{d-1}x_{\parallel}\left(\frac{c}{2}\Phi^2(z=0)-\mathbf{h}_1\cdot\Phi(z=0)+\frac{c}{2}\Phi^2(z=L)-\mathbf{h}_1\cdot\Phi(z=L)\right), \tag{2.1}$$

with space dimension d and position vector $\mathbf{x}=(\mathbf{x}_{\parallel},z)$ of $d-1$ parallel and one perpendicular components. The z integration extends over the interval $[0,L]$, where $z=0$ and $z=L$ give the positions of the film surfaces. τ is the temperature parameter such that in the bulk $\tau=0$ marks the transition temperature within mean-field theory. The coupling constant $g>0$ ensures the stability of the statistical weight below the transition temperature, i.e., for $\tau<0$. c denotes the surface enhancement, and $\mathbf{h}$ and $\mathbf{h}_1$ are bulk and surface fields, respectively. We focus on the ordinary transition at zero fields, i.e., we adopt the fixed point value $c=\infty$ for the surface enhancement and set $\mathbf{h}=\mathbf{h}_1=0$. After carrying out a Fourier transformation with respect to the $d-1$ directions exhibiting translational invariance parallel to the surfaces the mean-field propagator for the disordered phase ($\tau>0$) in the p-z representation is given by[48,70]

$$G_D(p,z_1,z_2,L,\tau)=\int d^{d-1}x_{\parallel}e^{i\mathbf{p}\cdot\mathbf{x}_{\parallel}}\langle\Phi(\mathbf{x}_{\parallel},z_1)\Phi(0,z_2)\rangle=\frac{1}{2b}\left(e^{-b|z_1-z_2|}-e^{-b(z_1+z_2)}+\frac{e^{-b(z_1-z_2)}+e^{-b(z_2-z_1)}-e^{-b(z_1+z_2)}-e^{b(z_1+z_2)}}{e^{2bL}-1}\right),\quad b=\sqrt{p^2+\tau}. \tag{2.2}$$

The first exponential function corresponds to the bulk part, followed by the contribution from the surface at $z=0$. Both exponentials together give the propagator for the ordinary transition of the semi-infinite system ($L=\infty$). The remaining ratio carries the L dependence. The propagator satisfies the Dirichlet boundary conditions $G_D(z=0)=0=G_D(z=L)$. Equation (2.2) represents the mean-field approximation for the two-point correlation function in the film corresponding to the critical behavior in $d=4$. The non-Gaussian fluctuations in $d=3$ are taken into account approximately by the one-loop correction, which amounts to the first term in a systematic expansion in terms of $\epsilon=4-d$:

$$G_{bare}(p,z_1,z_2,L,\tau,g)=G_D(p,z_1,z_2,L,\tau)-\frac{g}{2}\frac{n+2}{3}\int\frac{d^{d-1}q}{(2\pi)^{d-1}}\int_0^L dz\times G_D(p,z_1,z,L,\tau)G_D(q,z,z,L,\tau)\times G_D(p,z,z_2,L,\tau)+O(g^2). \tag{2.3}$$

As a regularization scheme we use a dimensional regularization by an analytic continuation in the space dimension $d=4-\epsilon$. As long as z_1 and z_2 are both off the surfaces, only bulk singularities occur. We absorb the corresponding poles in ϵ by minimal subtraction through the standard Z factors

$$\phi=Z_{\phi}^{1/2}\phi^R,\quad g=\mu^{\epsilon}2^d\pi^{d/2}Z_u u,\quad \tau=\mu^2 Z_t t, \tag{2.4}$$

where μ is the momentum scale, and the bulk Z factors are[71]

$$Z_{\phi}=1+O(u^2),\quad Z_u=1+\frac{n+8}{3}\frac{u}{\epsilon}+O(u^2),\quad Z_t=1+\frac{n+2}{3}\frac{u}{\epsilon}+O(u^2). \tag{2.5}$$

The renormalized correlation function reads [see Eq. (2.4)]

$$G(p,z_1,z_2,L,t,u;\mu)=Z_{\phi}^{-1}G_{bare}(p,z_1,z_2,L,\tau,g), \tag{2.6}$$

which is valid in all orders of perturbation theory. The solution of the corresponding renormalization-group equation leads to the following scaling property:

$$G(p,z_1,z_2,L,t;\mu)=\mathcal{G}_1 p^{-1+\eta}g_1(p\xi,z_1/\xi,z_2/\xi,L/\xi). \tag{2.7}$$

This holds at the fixed point $u^*=3\epsilon/(n+8)+O(\epsilon^2)$, and involves the bulk correlation length $\xi=\xi_0^+ t^{-\nu}$, the exponents $\eta=O(\epsilon^2)$, and $\nu=\frac{1}{2}+\frac{1}{4}[(n+2)/(n+8)]\epsilon+O(\epsilon^2)$. With a suitable normalization [see, cf., Eq. (2.13)] the scaling function g_1 is universal. The amplitude $\mathcal{G}_1$, which is fixed by this normalization, and the amplitude ξ_0^+ carry the nonuniversal scaling factors. We fix ξ_0^+ by defining ξ as the so-called true correlation length[72] so that $\xi_0^+=\mu^{-1}(1+\frac{1}{4}[(n+2)/(n+8)](1-C_E)\epsilon+O(\epsilon^2))$. This expression for ξ_0^+ allows one to express the momentum scale μ introduced in Eq. (2.4) in terms of the experimentally accessible, nonuniversal amplitude ξ_0^+:

$$\mu=(\xi_0^+)^{-1}\left(1+\frac{1}{4}\frac{n+2}{n+8}(1-C_E)\epsilon+O(\epsilon^2)\right). \tag{2.8}$$

If subsequent formulas contain the momentum scale μ explicitly it is to be replaced by Eq. (2.8); moreover we omit μ from the explicit list of variables of G.

Depending on the problem under consideration it is often advantageous to use different but equivalent representations of the correlation function such as

$$G(p,z_1,z_2,L,t)=\mathcal{G}_{\rm II}z_1^{1-\eta}g_{\rm II}(pz_2,z_1/\xi,z_2/\xi,z_2/L), \tag{2.9}$$

$$G(p,z_1,z_2,L,t)=\mathcal{G}_{\rm III}L^{1-\eta}g_{\rm III}(pz_1,z_1/L,z_2/L,L/\xi), \tag{2.10}$$

$$G(p,z_1,z_2,L,t)=\mathcal{G}_{\rm IV}\xi^{1-\eta}g_{\rm IV}(pL,pz_1,pz_2,\xi/L), \tag{2.11}$$

and

$$G(p,z_1,z_2,L,t) =\mathcal{G}_{\rm V}p^{-1+\eta}g_{\rm v}(p\xi,p(z_1-z_2),p(z_1+z_2),L/\xi). \tag{2.12}$$

The nonuniversal amplitudes $\mathcal{G}_x$ and the universal scaling functions g_x, $x=$I, II, III, IV, and V, are fixed by the following normalizations:

$$\lim_{\alpha\to\infty}\lim_{\beta\to\infty}\lim_{\delta\to\infty} g_{\rm I}(\alpha,\beta,\gamma=\beta,\delta)=1, \tag{2.13}$$

$$\lim_{\alpha\to 0}\lim_{\beta\to 0}\lim_{\delta\to 0} g_{\rm II}(\alpha,\beta,\gamma=\beta,\delta)=:g_{\rm II}(0,0,0,0)=1, \tag{2.14}$$

$$\lim_{\alpha\to 0}\lim_{\delta\to 0} g_{\rm III}(\alpha,\beta=1/2,\gamma=\beta=1/2,\delta)=1, \tag{2.15}$$

$$\lim_{\delta\to 0}\lim_{\alpha\to 0} g_{\rm IV}(\alpha,\beta=\alpha/2,\gamma=\beta=\alpha/2,\delta)=1, \tag{2.16}$$

and

$$\lim_{\beta\to 0}\lim_{\alpha\to\infty}\lim_{\gamma\to\infty}\lim_{\delta\to\infty} g_{\rm V}(\alpha,\beta,\gamma,\delta)=:g_{\rm V}(\infty,0,\infty,\infty)=1. \tag{2.17}$$

The universal scaling functions g_x can be expressed in terms of each other because, in Eqs. (2.7) and (2.9)–(2.12), the left-hand side is the same quantity and the sets of scaling variables are complete, i.e., from each set one can form any of the others by a suitable combination of variables.

Since the nonuniversal amplitudes $\mathcal{G}_x$ correspond to the same correlation function $G(p,z_1,z_2,L,t)$, and because the scaling functions fixed by the normalizations in Eqs. (2.13)–(2.17), are universal, their ratios $\mathcal{G}_x/\mathcal{G}_{x'}$ are universal numbers. Thus a knowledge of one of them and of the corresponding universal scaling functions determines all the others.

Moreover, as discussed in Appendix A, all nonuniversal amplitudes $\mathcal{G}_x$ are determined by any pair of nonuniversal scale factors which characterize the critical *bulk* properties. A transparent and experimentally directly accessible choice for the latter is the nonuniversal amplitude B of the leading temperature singularity of the field $\langle\phi(\mathbf{x})\rangle$ in the bulk below T_c,

$$\langle\phi(\mathbf{x})\rangle=B(-t)^{\beta}, \tag{2.18}$$

and the amplitude ξ_0^+ of the true correlation length above T_c. In terms of these quantities one has

$$\mathcal{G}_{\rm V}=B^2(\xi_0^+)^{d-2+\eta}\mathcal{U}, \tag{2.19}$$

where $\mathcal{U}$ is a universal number, whose value $\mathcal{U}\simeq 1.58$ is derived in Appendix A based on Eq. (2.17). In the following most of our analysis focuses on the scaling function $g_{\rm II}$ used in Eq. (2.9). For that case one finds (see Appendix A) the *universal* ratio

$$\mathcal{G}_{\rm II}/\mathcal{G}_{\rm V}=2\left(1+\epsilon\frac{n+2}{n+8}+O(\epsilon^2)\right). \tag{2.20}$$

With these results we finally obtain

$$G(p,z_1,z_2,L,t)=B^2(\xi_0^+)^{d-1}\mathcal{R}(z_1/\xi_0^+)^{1-\eta} \times g_{\rm II}(pz_2,z_1/\xi,z_2/\xi,z_2/L), \tag{2.21}$$

where $\mathcal{R}=2\mathcal{U}(1+\epsilon[(n+2)/(n+8)]+O(\epsilon^2))\simeq 4.21$ is a universal number. Thus in all our subsequent formulas for *film* properties their *absolute* values are determined and fixed by the two nonuniversal *bulk* amplitudes B and ξ_0^+.

The actual order parameter (OP) for a particular second-order phase transition is proportional to the field ϕ introduced in Eq. (2.1), i.e., $OP(\mathbf{x})=b\,\phi(\mathbf{x})$. The value of b depends on the particular system (binary alloy, liquid, ferromagnet etc.). Moreover, any rescaling of b by a dimensionless number renders another OP which is equally valid for describing the singular behavior of the phase transition. We emphasize that Eqs. (2.9), (2.19), and (2.20) remain valid if G is replaced by $\langle OP(\mathbf{x})OP(\mathbf{x}')\rangle$, $\langle\phi(\mathbf{x})\rangle$ by $\langle OP(\mathbf{x})\rangle$, and B by $B'=bB$; these replacements have to be carried out if the present field-theoretic results are used to interpret, e.g., the intensity of scattered x-rays or neutrons (see, c.f., Sec. IV). The actual choice of the OP, as it enters into the expression for the scattering cross section, is borne out and tight to the relation $\langle OP(\mathbf{x})\rangle=B'(-t)^{\beta}$.

III. EXPLICIT PROPERTIES OF THE TWO-POINT CORRELATION FUNCTION

The discussion of the correlation function consists of three parts. First we set $z_1=z_2$, and analyze its nonanalytic behavior in certain limits. Then we take into account the case $z_1\neq z_2$, which helps to understand the correlations perpendicular to the surfaces. Moreover, the discussion of this latter case turns out to be very useful for carrying out integrations appearing in the scattering cross section to be analyzed in Sec. IV. The film excess susceptibility is discussed in the last part of Sec. III.

A. Lateral two-point correlation function for $z_1=z_2$

In order to investigate various asymptotic properties of the lateral behavior of the two-point correlation function, we resort to short distance expansions (SDE's),[73] distant wall corrections,[59] and results of the perturbation theory supported by appropriate exponentiations of the explicit ϵ-expansion results. With $z_1=z_2=z$, in the present context a representation of the form

$$G(p,z,L,t)=\mathcal{G}_{\rm II}z^{1-\eta}g(pz,z/\xi,z/L) \tag{3.1}$$

is useful. According to Eq. (2.9), one has $g(u,v,w)=g_{\rm II}(u,v,v,w)$ with $g(0,0,0)=1$ [Eq. (2.14)]. For semi-infinite systems, i.e., $L=\infty$, the SDE in the cases $t=0$, $p\to 0$ and $p=0$, $t\to 0$[74,75] leads to the asymptotic behaviors

$$G(p,z,L=\infty,t=0)=\mathcal{G}_{\rm II}z^{1-\eta}g_1(u=pz)$$
$$\underset{p\to 0}{\to}\mathcal{G}_{\rm II}z^{1-\eta}[1+A_1(pz)^{-1+\eta_\parallel}+\cdots] \tag{3.2}$$

and

$$G(p=0,z,L=\infty,t)$$
$$=\mathcal{G}_{\rm II}z^{1-\eta}g_2(v=z/\xi)\underset{t\to 0}{\to}\mathcal{G}_{\rm II}z^{1-\eta}[1+B_1(z/\xi)^{-1+\eta_\parallel}+\cdots]$$
$$=\mathcal{G}_{\rm II}z^{1-\eta}[1+B_1(z/\xi_0^+)^{-1+\eta_\parallel}t^{-\gamma_{11}}+\cdots], \tag{3.3}$$

respectively, with $\gamma_{11}=\nu(\eta_\parallel-1)$, $g_1(u)=g(u,v=0,w=0)$, $g_1(0)=1$, $g_2(v)=g(u=0,v,w=0)$, and $g_2(0)=1$. In the case where $p=0$ and $t=0$, one has

$$G(p=0,z,L,t=0)=\mathcal{G}_{\rm II}z^{1-\eta}g_3(w=z/L), \tag{3.4}$$

with $g_3(w)=g(u=0,v=0,w)$ so that $g_3(0)=1$. In order to infer the first nontrivial dependence on L for $L\to\infty$, according to Eq. (3.4) one can equally consider the limit $z\to 0$ for L fixed. To this end we consider the SDE of the renormalized film correlation function in real space:

$$\langle\phi(\mathbf{x}_\parallel,z)\phi(0,z)\rangle\underset{z\to 0}{\to}\mu^{-2}(\mu z)^{2(x_s-x)}\langle\phi_\perp(\mathbf{x}_\parallel)\phi_\perp(0)\rangle$$
$$=\mu^{d-2}(\mu z)^{2(x_s-x)}(\mu x_\parallel)^{-2x_s}Y(x_\parallel/L) \tag{3.5}$$

Here $\phi_\perp$ denotes the normal derivate of ϕ taken at one of the surfaces, and $Y(y)$ is a dimensionless scaling function for the film which is universal up to a nonuniversal prefactor. The scaling dimensions of ϕ and $\phi_\perp$ are $x=\frac{1}{2}(d-2+\eta)$ and $x_s=\frac{1}{2}(d-2+\eta_\parallel)$, respectively. The scaling function $Y(x_\parallel/L)$ describes the influence of the distant wall at $z=L$ on the lateral correlations close to the near wall at $z=0$. In order to obtain its leading asymptotic behavior for $x_\parallel/L\to 0$, we use the identity

$$G(p=0,z,L,t=0)=G(p=0,z,L=\infty,t=0)$$
$$-\int_L^\infty\frac{\partial G(p=0,z,L',t=0)}{\partial L'}dL'. \tag{3.6}$$

The first term on the right-hand side is equal to $\mathcal{G}_{\rm II}z^{1-\eta}$ [compare Eqs. (3.2) and (3.3)]. The leading correction is given by using the SDE in Eq. (3.5) for the second term:

$$-\int_L^\infty\frac{\partial G(p=0,z,L',t=0)}{\partial L'}dL'=-\int d^{d-1}x_\parallel\int_L^\infty dL'\frac{\partial}{\partial L'}\langle\phi(\mathbf{x}_\parallel,z)\phi(0,z)\rangle$$
$$\underset{L\to\infty}{\to}-\int d^{d-1}x_\parallel\int_L^\infty dL'\frac{\partial}{\partial L'}\mu^{d-2}(\mu z)^{2(x_s-x)}(\mu x_\parallel)^{-2x_s}Y(x_\parallel/L')$$
$$=\mu^{-1}(\mu z)^{1-\eta}\left(\frac{z}{L}\right)^{-1+\eta_\parallel}\tilde{C} \tag{3.7}$$

with $\tilde{C}=[1/(\eta_\parallel-1)]\int d^{d-1}y\,y^{-(d-3+\eta_\parallel)}Y'(y)$. Thus we find $g_3(w\to 0)=1+C_1w^{-1+\eta_\parallel}$, where $C_1=\tilde{C}\mu^{-\eta}/\mathcal{G}_{\rm II}$ is a universal number, i.e.,

$$G(p=0,z,L\to\infty,t=0)=\mathcal{G}_{\rm II}z^{1-\eta}[1+C_1(z/L)^{-1+\eta_\parallel}+\cdots]. \tag{3.8}$$

Finally we note that due to the normalization $g(0,0,0)=1$ the scaling function $g(u,v,w)$ is given by the ratio $g(pz,z/\xi,z/L)=G(p,z,L,t)/G(p=0,z,L=\infty,t=0)$ from which the prefactors $\mathcal{G}_{\rm II}z^{1-\eta}$ appearing in Eq. (3.1) drop out. The ϵ expansions of the amplitudes of the leading asymptotic terms follow from Eqs. (B6), (B7), and (B8) in Appendix B 1:

$$A_1=-\left[1+\epsilon\frac{n+2}{n+8}(1-C_E-\ln 2)+O(\epsilon^2)\right],$$
$$B_1=-\left[1+\epsilon\frac{n+2}{n+8}(1-C_E)+O(\epsilon^2)\right], \tag{3.9}$$
$$C_1=-\left[1+\epsilon\frac{n+2}{n+8}\left(\frac{\pi^2}{18}-C_E+2(S_2+I_1)-1\right)+O(\epsilon^2)\right].$$

$C_E\approx 0.5772$ is Euler's constant, and $S_2\simeq 0.083$ and $I_1\simeq 0.287$ are given by Eq. (B9) in Appendix B1. Within the ϵ expansion the full forms of the scaling functions $g_1(u)$, $g_2(v)$, and $g_3(w)$ can be found in Appendix B1 [see Eqs. (B1) – (B3)].

In Fig. 1 we display the three scaling functions g_i, $i=1$, 2, and 3 [Eqs. (B1)–(B3)], corresponding to Eqs. (3.2), (3.3), and (3.4) as obtained within mean-field theory (MFT), i.e., for $\epsilon=0$, and from renormalization-group-guided perturbation theory (PT) as well as their leading behavior $g_i(x_i\to 0)=g_{i,l}(x_i)$, $x_1=u,x_2=v,x_3=w$. Within MFT the three scaling functions have the same limiting form for small scaling variables with $A_1=B_1=C_1=-1$ and the critical exponent $\eta_\parallel=2$. Beyond MFT, in Fig. 1 we use $\eta_\parallel=1.48$ as the best available estimate,[48] whereas the amplitudes are evaluated in first order in ϵ [Eq. (3.9) for $(n,\epsilon)=(1,1)$] so that

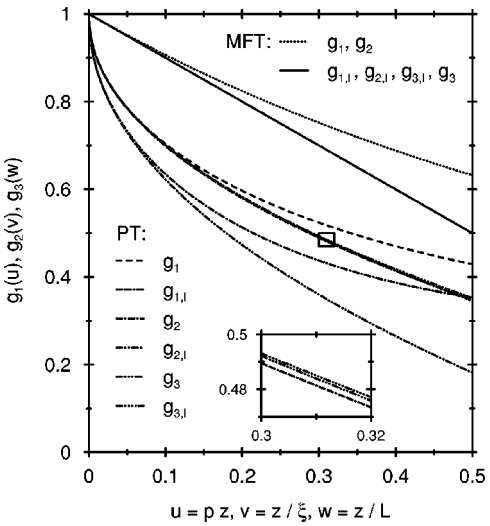

FIG. 1. The three scaling functions describing the lateral correlations $g(pz,z/\xi,z/L)$ in the film [Eq. (3.1)] for the limiting cases $p=0$, $\xi=\infty$, or $L=\infty$: $g_1(u=pz)\equiv g(pz,0,0)$ [$T=T_c, L=\infty$, Eq. (3.2)], $g_2(v=z/\xi)\equiv g(0,z/\xi,0)$ [$p=0, L=\infty$, Eq. (3.3)], and $g_3(w=z/L)\equiv g(0,0,z/L)$ [$p=0, T=T_c$, Eq. (3.4)]. The two uppermost curves correspond to the mean-field results for g_i, $i=1$, 2, and 3, and to their *l*eading behavior $g_i(x_i\to 0)=g_{i,l}(x_i)$, respectively, with $x_1=u$, $x_2=v$, and $x_3=w$; within MFT $g_1=g_2$, $g_{1,l}=g_{2,l}=g_{3,l}$, and $g_3=g_{3,l}$. The lower six curves correspond to $g_i(x_i)$ [Eqs. (B1), (B2), and (B3)] and $g_{i,l}(x_i)$ as obtained by *p*erturbation *t*heory for $d=3$. The difference between g_3 and $g_{3,l}$ is revealed only in the inset: $g_{1,l}(u)=1+A_1u^{-1+\eta_\parallel}$, $g_{2,l}(v)=1+B_1v^{-1+\eta_\parallel}$, and $g_{3,l}(w)=1+C_1w^{-1+\eta_\parallel}$. Within MFT one has $A_1=B_1=C_1=-1$ [Eq. (3.9)] and $\eta_\parallel=2$, whereas for $(n,d)=(1,3)$ PT yields $A_1\simeq -0.9099$, $B_1\simeq -1.1409$, $C_1\simeq -0.9035$, and $\eta_\parallel\simeq 1.48$. For vanishing scaling arguments all scaling functions attain 1.

$A_1\simeq -0.9099$, $B_1\simeq -1.1409$, and $C_1\simeq -0.9035$. Within mean-field theory $g_1=g_2$ and the leading asymptotic behavior $g_{3,l}$ provides already the full scaling function g_3. Beyond MFT there is a small difference between g_3 and $g_{3,l}$. This difference is much bigger for the scaling functions g_1 and g_2 describing the semi-infinite system.

The above discussion demonstrates that, for z fixed, the two-point correlation function $G(p,z,L,t)$ has a finite value $G(p=0,z,L=\infty,t=0)$ which is attained via cusplike singularities: $\sim p^{-1+\eta_\parallel}(p\to 0,1/L=0,t=0)$, $\sim(1/L)^{-1+\eta_\parallel}(1/L\to 0,p=0,t=0)$, and $\sim(1/\xi)^{-1+\eta_\parallel}(t\to 0,p=0,1/L=0)$. In terms of these variables the critical exponent is the same for all three cases and only the amplitudes differ. These singularities remain if only one out of the above three variables is zero and the remaining two both vanish. This behavior, which includes the smooth interpolation between the corresponding amplitudes, is described by the scaling functions h_1, h_2, and h_3 of two variables instead of the scaling functions with one variable as $g_1(u)$, $g_2(v)$, and $g_3(w)$:

$$G(p,z,L=\infty,t)=\mathcal{G}_{\rm II}z^{1-\eta}h_1(u,v),$$

$$h_1(u,v)=g(u,v,w=0), \tag{3.10}$$

$$G(p,z,L,t=0)=\mathcal{G}_{\rm II}z^{1-\eta}h_2(u,w),$$

$$h_2(u,w)=g(u,v=0,w), \tag{3.11}$$

and

$$G(p=0,z,L,t)=\mathcal{G}_{\rm II}z^{1-\eta}h_3(v,w),$$

$$h_3(v,w)=g(u=0,v,w), \tag{3.12}$$

with $u=pz$, $v=z/\xi$, and $w=z/L$. All three scaling function can be obtained from Eq. (B17). Since the discussion of all three scaling functions is analogous we demonstrate our analysis only for $h_3(v,w)$. We introduce the polar coordinates ω and φ,

$$\omega=\sqrt{v^2+w^2}=z\sqrt{\xi^{-2}+L^{-2}},$$

$$\varphi=\arctan(v/w)=\arctan(L/\xi), \quad v=\omega\sin\varphi, \tag{3.13}$$

$$w=\omega\cos\varphi,$$

which lead to

$$h_3(v,w)=h_3(\omega\sin\varphi,\omega\cos\varphi)=h^{(3)}_{polar}(\omega,\varphi). \tag{3.14}$$

Since the limit $\omega\to 0$, i.e., $1/\xi\to 0$ and $1/L\to 0$, is equivalent to the limit $z\to 0$ for ξ and L fixed the resulting singularity is compatible with the SDE, so that

$$h^{(3)}_{polar}(\omega\to 0,\varphi)=H^{(3)}_0(\varphi)+H^{(3)}_1(\varphi)\omega^{-1+\eta_\parallel}+\cdots. \tag{3.15}$$

The explicit form of the scaling function $h_3(v,w)$, as obtained from perturbation theory in $O(\epsilon)$, is in accordance with Eq. (3.15), and renders explicit results for the coefficients $H^{(3)}_0(\varphi)$ and $H^{(3)}_1(\varphi)$:

$$H_0(\varphi)=h^{(3)}_{polar}(\omega=0,\varphi)=h_3(v=0,w=0)=1 \tag{3.16}$$

is independent of φ and equal to 1 due to the normalization $g(u=0,v=0,w=0)=1$. With this result the ϵ expansion of $H^{(3)}_1(\varphi)$ follows by comparing the ϵ expansion of the right-hand side of Eq. (3.15) with the limit $\omega\to 0$ of the ϵ expansion of $h^{(3)}_{polar}(\omega,\varphi)$. As expected, one finds that $H^{(3)}_1(\varphi)$ interpolates smoothly between the value $H^{(3)}_1(\varphi=0)=C_1$ [see Eq. (3.9)] corresponding to the amplitude of the singularity $\sim(1/L)^{-1+\eta_\parallel}$ for $u=0$ and $v=0$ and the value $H^{(3)}_1(\varphi=\pi/2)=B_1$ [see Eq. (3.9)] corresponding to the amplitude of the singularity $\sim(1/\xi)^{-1+\eta_\parallel}$ for $u=0$ and $w=0$. In Fig. 2 all three amplitude functions $H^{(1)}_1(\varphi)$, $H^{(2)}_1(\varphi)$, and $H^{(3)}_1(\varphi)$ [see Eqs. (B10)–(B12)] are shown in MFT and in first order in ϵ (PT). Within MFT $H^{(1)}_1(\varphi)$ of the semi-infinite system is constant and $H^{(2)}_1(\varphi)=H^{(3)}_1(\varphi)$ exhibit a nontrivial dependence on φ. Beyond MFT all three functions interpolate between the amplitudes A_1, B_1, and C_1 [see Eq. (3.9)] in a nontrivial way.

In Figs. 3, 4, and 5 we display the full scaling functions $h_1(u,v)$, $h_2(u,w)$, and $h_3(v,w)$, respectively. In order to obtain such a scaling function beyond the leading asymptotic

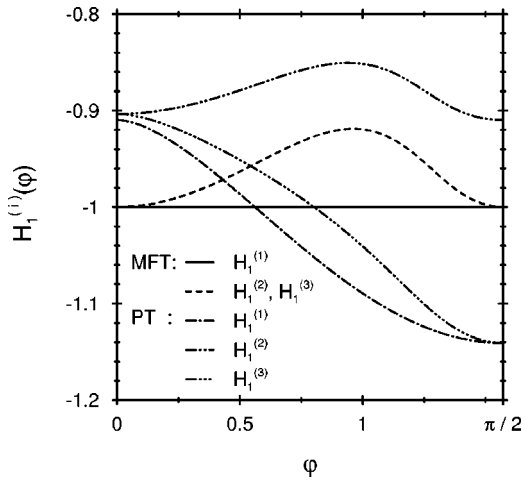

FIG. 2. $G(p\to 0,z,L=\infty,t\to 0)$, $G(p\to 0,z,L\to\infty,t=0)$, and $G(p=0,z,L\to\infty,t\to 0)$ attain their maximum value $G(p=0,z,L=\infty,t=0)=\mathcal{G}_{\Pi}z^{1-\eta}$ via cusplike singularities $H_1^{(1)}(\varphi)[z(p^2+\xi^{-2})^{1/2}]^{-1+\eta_\parallel}$ with $\varphi=\arctan[(p\xi)^{-1}]$, $H_1^{(2)}(\varphi)[z(p^2+L^{-2})^{1/2}]^{-1+\eta_\parallel}$ with $\varphi=\arctan(pL)$, and $H_1^{(3)}(\varphi)[z(\xi^{-2}+L^{-2})^{1/2}]^{-1+\eta_\parallel}$ with $\varphi=\arctan(L/\xi)$, respectively, interpolating smoothly between the singularity $A_1(pz)^{-1+\eta_\parallel}$ for $(t=0,L=\infty)$ and $B_1(z/\xi)^{-1+\eta_\parallel}$ for $(p=0,L=\infty)$, $C_1(z/L)^{-1+\eta_\parallel}$ for $(p=0,t=0)$ and $A_1(pz)^{-1+\eta_\parallel}$ for $(L=\infty,t=0)$, and $C_1(z/L)^{-1+\eta_\parallel}$ for $(t=0,p=0)$ and $B_1(z/\xi)^{-1+\eta_\parallel}$ for $(L=\infty,p=0)$, respectively. In $O(\epsilon)$ of PT, the amplitude functions $H_1^{(i)}(\varphi)$, $i=1$, 2, and 3, are given by Eqs. (B10), (B11), and (B12). In $O(\epsilon)$ one has $H_1^{(1)}(0)=H_1^{(2)}(\pi/2)=A_1\simeq -0.9099$, $H_1^{(1)}(\pi/2)=H_1^{(3)}(\pi/2)=B_1\simeq -1.1409$, and $H_1^{(2)}(0)=H_1^{(3)}(0)=C_1\simeq -0.9035$. Within MFT $H_1^{(i)}(\varphi=0)=H_1^{(i)}(\varphi=\pi/2)=-1$ and $H_1^{(1)}(\varphi)$ is constant; moreover $H_1^{(2)}(\varphi)=H_1^{(3)}(\varphi)$ but not constant.

form we first subtract its leading contribution in its ϵ-expanded form in $O(\epsilon)$ from the full expression of the scaling function, and add the leading exponentiated contribution afterwards. This exponentiation scheme is consistent with the explicit expanded form up to and including $O(\epsilon)$. In Figs. 6, 7, and 8, we show cross sections of the three-dimensional plots in order to illustrate the emergence of the

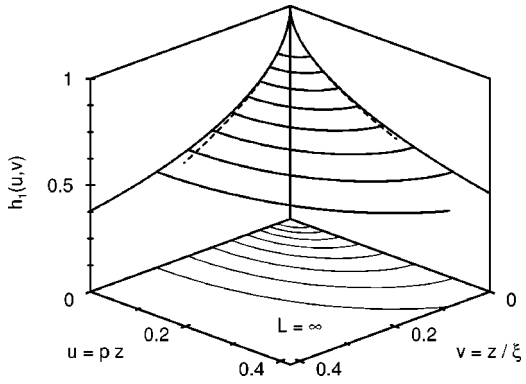

FIG. 3. The exponentiated scaling function $h_1(u=pz,v=z/\xi)$ [Eq. (3.10)] corresponding to the case $L=\infty$. We show the contour lines $h_1(u,v)=h_{polar}^{(1)}[\omega=(u^2+v^2)^{1/2},\varphi=\arctan(v/u)]$ for $h_1=0.8$, 0.75, 0.7, 0.65, 0.6, 0.55, 0.5, and 0.45, with their projections onto the uv plane as well as $h_1(u,v=0)=g_1(u)$ [Eq. (3.2)] and $h_1(u=0,v)=g_2(v)$ [Eq. (3.3)], which are discussed in Fig. 1. The dashed lines correspond to the leading singularities $g_1(u\to 0)=1+A_1u^{-1+\eta_\parallel}$ and $g_2(v\to 0)=1+B_1v^{-1+\eta_\parallel}$, respectively.

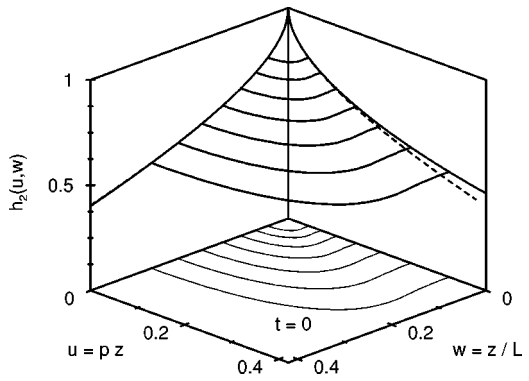

FIG. 4. The exponentiated scaling function $h_2(u=pz,w=z/L)$ [Eq. (3.11)] at bulk criticality $t=0$. We show the contour lines $h_2(u,w)=h_{polar}^{(2)}[\omega=(u^2+w^2)^{1/2},\varphi=\arctan(u/w)]$ for $h_2=0.8$, 0.75, 0.7, 0.65, 0.6, 0.55, and 0.5 with their projections onto the uw plane as well as $h_2(u,w=0)=g_1(u)$ [Eq. (3.2)] and $h_2(u=0,w)=g_3(w)$ [Eq. (3.4)]. The dashed lines correspond to the leading singularities $g_1(u\to 0)=1+A_1u^{-1+\eta_\parallel}$ and $g_3(w\to 0)=1+C_1w^{-1+\eta_\parallel}$, respectively. In the latter case the difference between the leading behavior and the full scaling function $g_3(w)$ is hardly visible. Thus the leading dependence on z/L for $p=0$, $t=0$ remains valid nearly up to the middle of the film at $z/L=0.5$.

$p^{-1+\eta_\parallel}$ cusplike singularity upon varying t or L, the $(1/\xi)^{-1+\eta_\parallel}$ cusplike singularity upon varying p or L, and the $(1/L)^{-1+\eta_\parallel}$ cusplike singularity upon varying t or p, respectively.

B. Perpendicular correlations

In a semi-infinite system the perpendicular correlations in real space define the exponent $\eta_\perp=(\eta+\eta_\parallel)/2$ through the limit $G(x_\parallel,z_1\to\infty,z_2,L=\infty,t)\sim z_1^{-(d-2+\eta_\perp)}$ with $x_\parallel$ and z_2 fixed. A Fourier transformation leads to the relation $G(p=0,z_1,z_2,L=\infty,t)\sim z_1^{1-\eta_\perp}$ with z_2 fixed and $z_1\to\infty$.

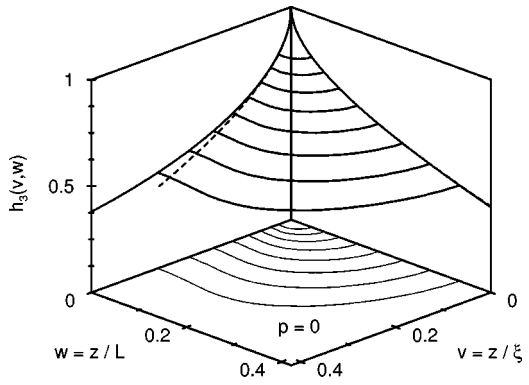

FIG. 5. The exponentiated scaling function $h_3(v=z/\xi,w=z/L)$ [Eq. (3.12)] for lateral momentum $p=0$. We show the contour lines $h_3(v,w)=h_{polar}^{(3)}[\omega=(v^2+w^2)^{1/2},\varphi=\arctan(v/w)]$ for $h_3=0.8$, 0.75, 0.7, 0.65, 0.6, 0.55, 0.5, and 0.45 with their projections onto the vw plane as well as $h_3(v,w=0)=g_2(v)$ [Eq. (3.3)] and $h_3(v=0,w)=g_3(w)$ [Eq. (3.4)]. The dashed lines correspond to the leading singularities $g_2(v\to 0)=1+B_1v^{-1+\eta_\parallel}$ and $g_3(w\to 0)=1+C_1w^{-1+\eta_\parallel}$, respectively. In the latter case the difference between the leading behavior and the full scaling function $g_3(w)$ is hardly visible. Thus the leading dependence on z/L for $p=0$ and $t=0$ remains valid nearly up to the middle of the film at $z/L=0.5$.

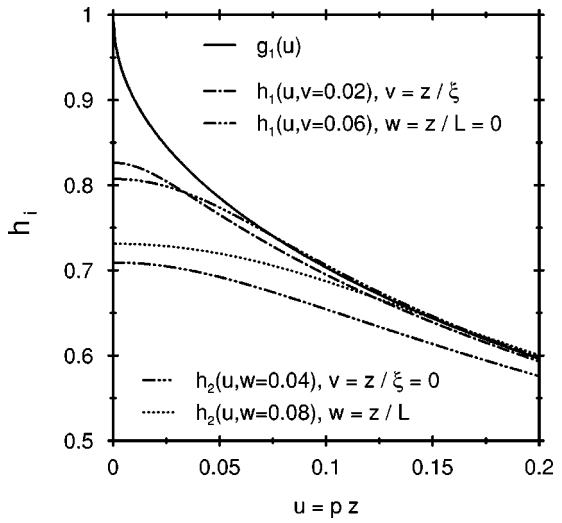

FIG. 6. The scaling function $g_1(u=pz)$ [Eq. (3.2)] with the cusplike singularity $g_1(u\to 0)= 1+A_1u^{-1+\eta_\parallel}$ evolves out of the scaling functions $h_1(u,v=z/\xi)$ [Eq. (3.10)] and $h_2(u,w=z/L)$ [Eq. (3.11)] in the limits $v\to 0$ and $w\to 0$, respectively, which are analytic functions of u, with a maximum at $u=0$, for $v\neq 0$ or $w\neq 0$. The various curves correspond to vertical cuts of the surface shown in Fig. 3 for $v=$const with $w=z/L=0$ and in Fig. 4 for $w=$const with $v=z/\xi=0$, respectively.

Note that in real space $G(x_\parallel,z_1,z_2,L=\infty,t=0)$ *increases* as function of z_1 for z_2 and $x_\parallel$ fixed, reaches a maximum at a certain value $z_1^*=z_2 f(x_\parallel/z_2)$ and finally vanishes for $z_1\to\infty$. This increase for $0<z_1<z_1^*$ leads to the divergence $\sim z_1^{1-\eta_\perp}$, $1-\eta_\perp\simeq 0.25$, of $G(p=0,z_1,z_2,L=\infty,t=0)=\int dx_\parallel\langle\phi(0,z_1)\phi(x_\parallel,z_2)\rangle$. The coordinates z_1 and z_2 can be interchanged. Actually conformal invariance fixes completely the functional form of $G(p=0,z_1,z_2,L=\infty,t=0)$ (see Ref. 76). The SDE leads up to a constant amplitude to the expression

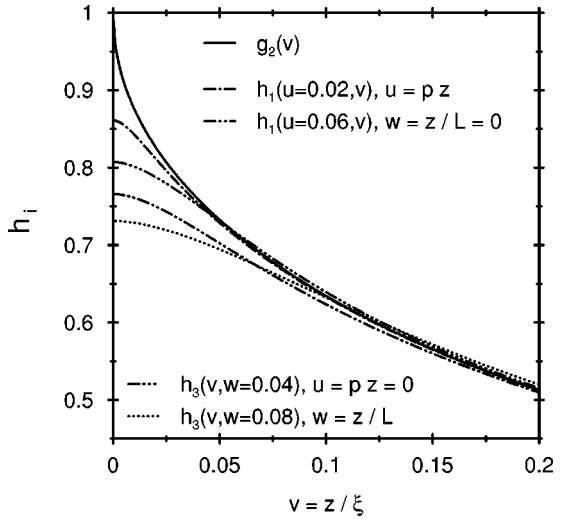

FIG. 7. The scaling function $g_2(v=z/\xi)$ [Eq. (3.3)] with the cusplike singularity $g_2(v\to 0)=1+B_1v^{-1+\eta_\parallel}$ evolves out of the scaling functions $h_1(u=pz,v)$ [Eq. (3.10)] and $h_3(v,w=z/L)$ [Eq. (3.12)] in the limits $u\to 0$ and $w\to 0$, respectively, which are analytic functions of v, with a maximum at $v=0$, for $u\neq 0$ or $w\neq 0$. The various curves correspond to vertical cuts of the surface shown in Fig. 3 for $u=$const with $w=z/L=0$ and in Fig. 5 for $w=$const with $u=pz=0$, respectively.

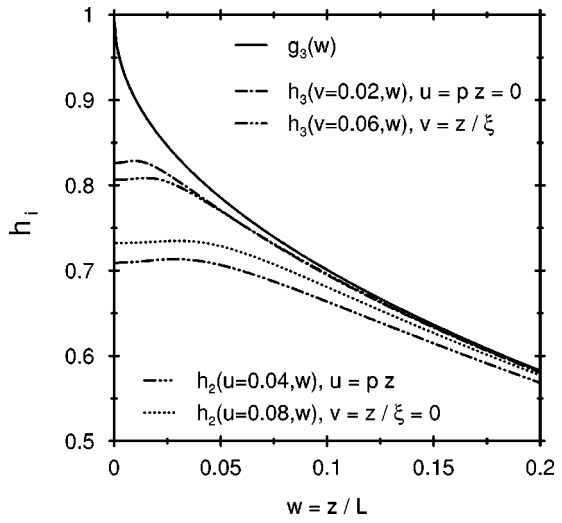

FIG. 8. The scaling function $g_3(w=z/L)$ [Eq. (3.4)] with the cusplike singularity $g_3(w\to 0)= 1+C_1w^{-1+\eta_\parallel}$ evolves out of the scaling functions $h_3(v=z/\xi,w)$ [Eq. (3.12)] and $h_2(u=pz,w)$ [Eq. (3.11)] in the limits $v\to 0$ and $u\to 0$, respectively, which are analytic functions of w for $u\neq 0$ or $w\neq 0$. The various curves correspond to vertical cuts of the surface shown in Fig. 5 for $v=$const with $pz=0$ and in Fig. 4 for $u=$const with $z/\xi=0$. We note that, different from Figs. 6 and 7, the scaling functions $h_3(v\neq 0,w)$ and $h_2(u\neq 0,w)$ are nonmonotonous functions and exhibit a maximum at $w\neq 0$ and a local minimum at $w=0$.

$$G(p=0,z_1,z_2,L=\infty,t=0)\sim(z_1z_2)^{(1-\eta)/2}\left(\Theta(z_1-z_2)\frac{z_2}{z_1}+\Theta(z_2-z_1)\frac{z_1}{z_2}\right)^{(\eta_\parallel-1)/2}+\cdots \tag{3.17}$$

[see Eq. (4.68) in Ref. 77]. The explicit calculation to first order in ϵ gives

$$G(p=0,z_1,z_2,L=\infty,t=0)=\mathcal{G}_{\rm II}(z_1z_2)^{(1-\eta)/2}\left(\Theta(z_1-z_2)\frac{z_2}{z_1}+\Theta(z_2-z_1)\frac{z_1}{z_2}\right)^{(\eta_\parallel-1)/2} \tag{3.18}$$

for arbitrary z_1 and z_2. This perturbation theory guided result for $d=3$ has a structure similar to the exact result from conformal theory in $d=2$ (see Refs. 76 and 77). Therefore, one is led to the conclusion that Eq. (3.18) is a good approximation for the exact correlation function in $d=3$. Guided by these considerations we find that in the case that the variables p, t, and $1/L$ are small but nonzero, the explicit results for G obtained from the ϵ expansion can be cast into the following forms:

$$G(p\to 0,z_1,z_2,L=\infty,t=0)$$
$$=\mathcal{G}_{\rm II}\Bigg[\Theta(z_2-z_1)z_1^{1-\eta}\left(\frac{z_2}{z_1}\right)^{1-\eta_\perp}\times[1+A_1(pz_2)^{-1+\eta_\parallel}+\cdots]+\Theta(z_1-z_2)z_2^{1-\eta}\left(\frac{z_1}{z_2}\right)^{1-\eta_\perp}\times[1+A_1(pz_1)^{-1+\eta_\parallel}+\cdots]\Bigg], \quad (3.19)$$

$$G(p=0,z_1,z_2,L=\infty,t\to 0)$$
$$=\mathcal{G}_{\rm II}\Bigg\{\Theta(z_2-z_1)z_1^{1-\eta}\left(\frac{z_2}{z_1}\right)^{1-\eta_\perp}\times\left[1+B_1\left(\frac{z_2}{\xi}\right)^{-1+\eta_\parallel}+\cdots\right]+\Theta(z_1-z_2)z_2^{1-\eta}\left(\frac{z_1}{z_2}\right)^{1-\eta_\perp}\times\left[1+B_1\left(\frac{z_1}{\xi}\right)^{-1+\eta_\parallel}+\cdots\right]\Bigg\}, \quad (3.20)$$

and

$$G(p=0,z_1,z_2,L\to\infty,t=0)$$
$$=\mathcal{G}_{\rm II}\Bigg\{\Theta(z_2-z_1)z_1^{1-\eta}\left(\frac{z_2}{z_1}\right)^{1-\eta_\perp}\times\left[1+C_1\left(\frac{z_2}{L}\right)^{-1+\eta_\parallel}+\cdots\right]+\Theta(z_1-z_2)z_2^{1-\eta}\left(\frac{z_1}{z_2}\right)^{1-\eta_\perp}\times\left[1+C_1\left(\frac{z_1}{L}\right)^{-1+\eta_\parallel}+\cdots\right]\Bigg\}. \quad (3.21)$$

These expressions are valid for arbitrary z_1 and z_2 as long as the scaling variables $pz_{1,2}$, $z_{1,2}/\xi$, and $z_{1,2}/L$ are small. The explicit ϵ expansion provides the amplitudes A_1, B_1, and C_1 given by Eq. (3.9). For the special case $z_1=z_2$, Eqs. (3.19)–(3.21) reduce to Eqs. (3.2), (3.3), and (3.8). In the limits $p=0$, $t=0$, and $L=\infty$, Eqs. (3.19)–(3.21) reduce to Eq. (3.17) [recall $\eta_\perp=(\eta_\parallel+\eta)/2$].

Finally we note that Eqs. (3.19), (3.20), and (3.21), and the full film correlation function $G(p,z_1,z_2,L,t)$ up to first order in ϵ [see Eq. (B17) in Appendix B 2], satisfy the so-called product rule derived by Parry and Swain for the correlation function algebra of inhomogeneous fluids [see Eq. (2.20) in Ref. 78]:

$$G(p,z_1,z_2,L,t)G(p,z_2,z_3,L,t)=G(p,z_2,z_2,L,t)G(p,z_1,z_3,L,t) \quad (3.22)$$

for all $0<z_1\leqslant z_2\leqslant z_3<L$. The second identity derived by Parry and Swain [see Eq. (2.21) in Ref. 78] is trivially fulfilled in the disordered phase considered here because it involves the derivative of the order-parameter profile which vanishes above T_c. A nontrivial test of this relation would require results for the ordered phase below T_c.

C. Susceptibility

As became apparent in Sec. III B, the full dependence of the correlation function G on all its variables p, z_1, z_2, L, and t is rather complicated. Therefore, it increases the clarity to consider a spatially averaged quantity which still displays interesting specific properties of the critical behavior in a film geometry. The singular part of the total susceptibility per area defined as

$$\chi(L,t)=\int_0^L dz_1\int_0^L dz_2 G(p=0,z_1,z_2,L,t) \quad (3.23)$$

provides such a reduced but still interesting quantity in that it depends only on two variables L and t. In addition, this susceptibility is directly accessible in an experiment which probes the response of a thin magnetic film on the applied external field in the limit of vanishing field strength.

From the scaling properties for G one obtains the following scaling property for χ [see Eqs. (2.21) and (A11)]:

$$\chi(L,t)=B^2(\xi_0^+)^{d+1}\left(\frac{L}{\xi_0^+}\right)^{3-\eta}\mathcal{R}f(y=L/\xi)=L^{3-\eta}\mathcal{G}_{\rm II}f(y), \quad (3.24)$$

where

$$f(y)=\int_0^1 dx_1\int_0^1 dx_2 x_1^{1-\eta}g_{\rm II}(0,x_1y,x_2y,x_2) \quad (3.25)$$

is a universal scaling function. For $y\to\infty$, i.e., $L\to\infty$ and t fixed the scaling function $f(y)$ vanishes as follows:

$$f(y\to\infty)=\mathcal{A}y^{-2+\eta}+\mathcal{B}y^{-3+\eta}+\mathcal{C}y^{-3+\eta}e^{-y}+O(e^{-2y}) \quad (3.26)$$

with

$$\mathcal{A}=1-\tilde{\epsilon}+O(\epsilon^2),$$
$$\mathcal{B}=-2\left\{1+\tilde{\epsilon}\left[\pi\left(\frac{1}{2}-\frac{1}{\sqrt{3}}\right)-1\right]\right\}+O(\epsilon^2), \quad (3.27)$$
$$\mathcal{C}=4\left\{1-\tilde{\epsilon}\left[\frac{\pi}{2}\left(1-\frac{1}{\sqrt{3}}\right)+1\right]\right\}+O(\epsilon^2),$$

so that, with $\gamma=\nu(2-\eta)$ and $\gamma_s=\gamma+\nu$,

$$\chi(L\to\infty,t)=B^2(\xi_0^+)^{d+1}\mathcal{R}\left\{\frac{L}{\xi_0^+}\mathcal{A}t^{-\gamma}+\mathcal{B}t^{-\gamma_s}\times\left[1+\frac{\mathcal{C}}{\mathcal{B}}e^{-L/\xi}+O(e^{-2L/\xi})\right]\right\}. \quad (3.28)$$

The first term ($\sim t^{-\gamma}$) corresponds to the bulk contribution of the total susceptibility. (We recall that χ is the total susceptibility per area $A_\parallel$ of one surface and that the total volume of the system is $A_\parallel L$.) The universal amplitude $\mathcal{A}$ [Eq.

(3.27)] is in accordance with the corresponding known universal amplitude ratios.[79,80] The second term ($\sim t^{-\gamma_s}$) corresponds to the sum of the excess susceptibilities of two semi-infinite systems within the surface universality class of the ordinary transition resembling the two bounding surfaces of the film. The corresponding universal amplitude $\mathcal{B}$ [Eq. (3.27)] of the semi-infinite systems is in accordance with the corresponding result in Ref. 81. Finally, the last term $\sim e^{-L/\xi}$ in Eq. (3.28) is the actual finite-size contribution induced by the finite distance L between the two surfaces confining the film. It is interesting to note that the structure of this finite-size term $\mathcal{C}t^{-\gamma_s}\exp(-L/\xi)$ differs from its counterparts for the free energy and specific heat in two respects [see Eqs. (4.8) and (6.14) in Ref. 30(a)]: (i) For ordinary-ordinary boundary conditions the finite size terms of the latter two both vanish $\sim\exp(-2y)$ for large $y=L/\xi$. (ii) The prefactor $\mathcal{C}t^{-\gamma_s}$ is replaced by $\mathcal{C}'t^{-\kappa}y^{\kappa/(2\nu)}$ with $\kappa=\alpha_s-2$ (free energy) and $\kappa=\alpha_s=\alpha+\nu$ (specific heat), respectively. From the explicit result in $O(\epsilon)$ we infer that in the case of the excess susceptibility this power law in front of the exponential is either missing or has an exponent of $O(\epsilon^2)$. In order to make clearer the comparison between the finite-size scaling of the free energy and specific heat on one hand, and the susceptibility on the other hand, we rewrite the susceptibility as

$$\chi(L,t)=B^2(\xi_0^+)^{d+1}\mathcal{R}\left(\frac{L}{\xi_0^+}\right)^{\gamma_s/\nu}\{\mathcal{A}y^{-\gamma/\nu}+\mathcal{B}y^{-\gamma_s/\nu}+g(y)\} \tag{3.29}$$

where $(2-\eta=\gamma/\nu,\ 3-\eta=\gamma_s/\nu)$

$$g(y)=f(y)-\mathcal{A}y^{-2+\eta}-\mathcal{B}y^{-3+\eta}. \tag{3.30}$$

The finite-size scaling for the singular part $\mathcal{F}_{sing}$ of the free energy of a film has a similar form $[d=(2-\alpha)/\nu,\ d-1=(2-\alpha_s)/\nu]$ [see Eq. (4.11) in Ref. 30(a)]

$$\frac{\mathcal{F}_{sing}}{k_bT_c(\infty)}=\frac{A_\parallel}{(\xi_0^+)^{d-1}}\left(\frac{L}{\xi_0^+}\right)^{(\alpha_s-2)/\nu}\times\{A_by^{-(\alpha-2)/\nu}+A_sy^{-(\alpha_s-2)/\nu}+\Theta(y)\}. \tag{3.31}$$

$A_\parallel$ is the area of the cross section of the film. In both Eqs. (3.29) and (3.31) the first two terms correspond to the bulk and surface contributions, respectively. In both cases the curly bracket represents a universal scaling function. For the susceptibility the finite-size part vanishes as

$$g(y\to\infty)=\mathcal{C}y^{-\gamma_s/\nu}e^{-y}+O(e^{-2y}) \tag{3.32}$$

whereas for the free energy one has

$$\Theta(y\to\infty)=\mathcal{C}'y^{-(\alpha_s-2)/(2\nu)}e^{-2y}+O(e^{-3y}). \tag{3.33}$$

At this point we note that the film susceptibility has also been discussed by Nemirovsky and Freed [see Eqs. (3.14d) and (3.16d) in Ref. 68]. Instead of the (p,z_1,z_2) representation of the propagator employed here, they used a discrete spectral $(p\text{-}\kappa_j)$ representation. In the discrete representation the propagator for Dirichlet boundary conditions is given by

$$G_{D,j}(p,\tau)=\frac{1}{p^2+\tau+\kappa_j^2},\quad \kappa_j=\pi(j+1)/L,\quad j=0,1,2,\ldots. \tag{3.34}$$

The (p,z_1,z_2) and $(p\text{-}\kappa_j)$ representations are related by the formula

$$G_D(p,z_1,z_2,L,\tau)=\frac{2}{L}\sum_{j=0}^{\infty}\sin(\kappa_jz_1)\sin(\kappa_jz_2)G_{D,j}(p,\tau). \tag{3.35}$$

The one-loop contribution to the total susceptibility is given by

$$\begin{aligned}-\frac{g}{2}\frac{n+2}{3}\int_0^L dz_1\int_0^L dz_2\int\frac{d^{d-1}q}{(2\pi)^{d-1}}\int_0^L dz\,G_D(p=0,z_1,z,L,\tau)G_D(q,z,z,L,\tau)G_D(p=0,z,z_2,L,\tau)\\ =-\frac{g}{2}\frac{n+2}{3}\int_0^L dz_1\int_0^L dz_2\int\frac{d^{d-1}q}{(2\pi)^{d-1}}\int_0^L dz\left(\frac{2}{L}\right)^3\sum_{m_1,m_2,m_3=0}^{\infty}\\ \times\sin(\kappa_{m_1}z_1)\sin(\kappa_{m_1}z)G_{D,m_1}(p=0,\tau)\sin^2(\kappa_{m_2}z)G_{D,m_2}(q,\tau)\sin(\kappa_{m_3}z)\sin(\kappa_{m_3}z_2)G_{D,m_3}(p=0,\tau).\end{aligned} \tag{3.36}$$

After performing the integrations, one has to evaluate the triple sum. In their calculation of the susceptibility Nemirovsky and Freed omitted the terms $m_1\neq m_3$ in the above sum, which leads to an erroneous expression for the scaling function $f(y)$. If, however, all terms in the triple sum are properly taken into account, one obtains, as expected, the same correct result for $f(y)$ as via the (p,z_1,z_2) representation.

The above discussion focused on the limit $y=L/\xi\to\infty$, i.e., on increasing the film thickness at a fixed temperature. In the opposite limit $y\to0$ the film thickness is kept fixed and one approaches the bulk critical temperature $T_c(L=\infty)$, where ξ diverges as $\xi_0^+\{[T-T_c(L=\infty)]/T_c(L=\infty)\}^{-\nu}$. For Dirichlet boundary conditions, as considered here, the critical temperature of the film occurs at a lower temperature $T_c(L)<T_c(L=\infty)$. Therefore, the film is not critical at $T_c(L=\infty)$, and thus the susceptibility is an analytic function of t around $t=[T-T_c(L=\infty)]/T_c(L=\infty)=0$. Therefore, the finite-size scaling function $g(y\to0)$ has the form

$$g(y\to0)=-\mathcal{A}y^{-\gamma/\nu}-\mathcal{B}y^{-\gamma_s/\nu}+\mathcal{D}+\mathcal{E}y^{1/\nu}+O(y^{2/\nu}), \tag{3.37}$$

with

$$\mathcal{D}=\frac{1}{12}\left[1-\tilde{\epsilon}\left(\frac{\pi^2}{60}+12b_2+1\right)\right]+O(\epsilon^2) \qquad (3.38)$$

and

$$\mathcal{E}=-\frac{1}{120}\left[1+\tilde{\epsilon}\left(4a_2-\frac{17\pi^2}{504}+102b_4-10b_2-1\right)\right]+O(\epsilon^2), \qquad (3.39)$$

so that

$$f(y\to 0)=\mathcal{D}+\mathcal{E}y^{1/\nu}+O(y^{2/\nu}). \qquad (3.40)$$

The numbers a_2, b_2, and b_4 are given in Eq. (B26) in Appendix B 3. For $(n,d)=(1,3)$ the values of the amplitudes to first order in ϵ are $\mathcal{D}\simeq 0.081\,42$ and $\mathcal{E}\simeq -0.013\,75$; for $\mathcal{A}$ and $\mathcal{B}$, see Eq. (3.27). The explicit form of the scaling function and its limiting behaviors are given in Appendix B 3. Figure 9(a) shows $f(y)$ within mean-field theory and within perturbation theory in first order ϵ as well as its corresponding asymptotic behaviors for large and small values of y; Fig. 9(b) displays $g(y)$ for large values of y.

Our investigations are restricted to temperatures $T\geqslant T_c$. Recently Leite, Sardelich, and Coutinho-Filho (LSC)[82] analyzed amplitude ratios of the specific heat and the susceptibility above $(T>T_c)$ and below $(T<T_c)$ the bulk critical temperature in the parallel plate geometry for various boundary conditions. These amplitude ratios are functions of the scaling variable $L/\xi_{\pm}$ [where $\xi_{\pm}$ is the correlation length above $(+)$ and below $(-)$ the bulk critical temperature], and describe the surface excess and finite-size contributions of the system. Their result for the amplitude function of the susceptibility above T_c [see the expression for C_+ in Eq. (22) in Ref. 82] can be expressed in terms of the scaling function $f(y)$ as introduced in Eq. (3.24). Within this framework the results of LSC to first order in ϵ for Dirichlet boundary conditions are equivalent to the following version of the scaling function $f(y)$:

$$f_{LSC}(y)=y^{-2}\left[1-\frac{\epsilon}{3}+\frac{\epsilon}{3}\int_0^1 ds\, f_{1/2}\left(\sqrt{s}\,\frac{y}{\pi}\right)-\frac{\epsilon\pi}{6y}\right]+O(\epsilon^2), \qquad (3.41)$$

with

$$f_{1/2}(a)=\int_a^{\infty}\frac{(u^2-a^2)^{-1/2}du}{\exp(2\pi u)-1}. \qquad (3.42)$$

For small values of the scaling variable y, this scaling function $f_{LSC}(y)$ deviates even within mean-field theory *qualitatively* from the actual correct form $f(y)$ given in Eqs. (B23) and (3.40). Moreover, for $y\lesssim 10$ the difference between f_{LSC} and f becomes larger than 10% in $O(\epsilon)$ and larger than 25% within mean-field theory. These discrepancies are due to the fact that even within mean-field theory the results of LSC do not reproduce the correct surface excess contributions[81] and finite-size contribution [Eq. (B23)].

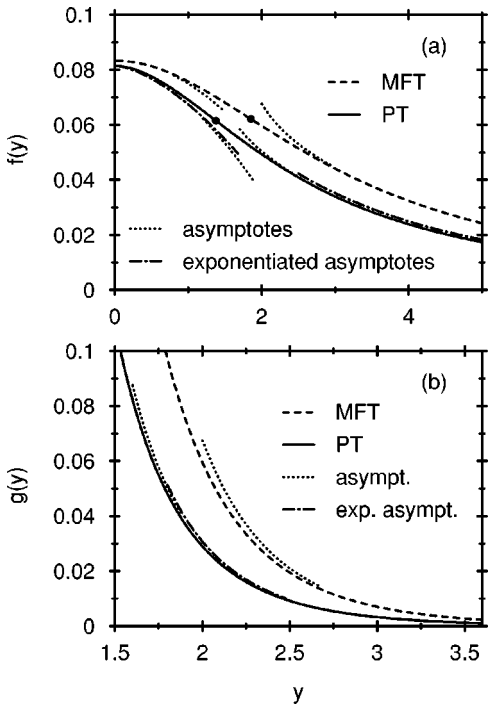

FIG. 9. Universal scaling functions $f(y)$ (a) [Eq. (3.24)] and $g(y)$ (b) [Eqs. (3.29) and (3.30)] of the film susceptibility for Dirichlet boundary conditions at both surfaces. The dashed lines are the MFT results, whereas the full lines include non-Gaussian fluctuations obtained by PT in first order ϵ [Eqs. (B22), (B23), and (3.30)]. The dotted lines indicate the asymptotic behaviors of $f(y\to 0)$, $f(y\to\infty)$, $g(y\to 0)$, and $g(y\to\infty)$ given by Eqs. (3.40), (3.26), (3.37), and (3.32), respectively. The dotted lines correspond to the ϵ expansion of these asymptotic behaviors up to $O(\epsilon)$ in order to be compatible with the full scaling functions $f(y)$ and $g(y)$, whose ϵ expansions up to $O(\epsilon)$ are shown here as full lines. The dash-dotted curves show the exponentiated forms of the asymptotic behaviors given by Eqs. (3.40), (3.26), (3.37), and (3.32) using the ϵ-expansion results for the amplitudes but the best available numbers $\eta=0.031$ and $\nu=0.630$ for the critical exponents. $f(y)$ has a turning point (●) at $y=1.851$ in MFT and at $y=1.376$ in $O(\epsilon)$; $f(0)=\mathcal{D}$ [Eq. (3.38)].

IV. SCATTERING CROSS SECTION

A. Scattering theory

As pointed out in Sec. I the diffuse scattering of x rays and neutrons under grazing incidence allows one to probe the local structure factor near interfaces and in thin films. In this section we discuss how the singularities of the two-point correlation function near criticality in a film, as calculated above, translate into singularities of the diffuse scattering intensity under the aforementioned experimental conditions.

We consider a film $(0\leqslant z\leqslant L)$ composed of a material 2 sandwiched in between two half-spaces filled with materials 1 $(z<0)$ and 3 $(z>L)$, respectively (see Fig. 10). An incoming plane wave of x rays or neutrons with momentum $\mathbf{K}^i=(\mathbf{k}_i,q_i)$ impinges on the 1-2 interface at an angle of incidence α_i so that $q_i=K^i\sin\alpha$ and $\mathbf{k}_i=K^i\cos\alpha_i(\cos\varphi_i,\sin\varphi_i,0)$. $\lambda=2\pi/K^i$ is the wavelength of the x rays or neutrons. We assume that media 1 and 3 are homogeneous, and that the 1-2 and 2-3 interfaces are laterally flat so that their contributions to diffuse scattering can be

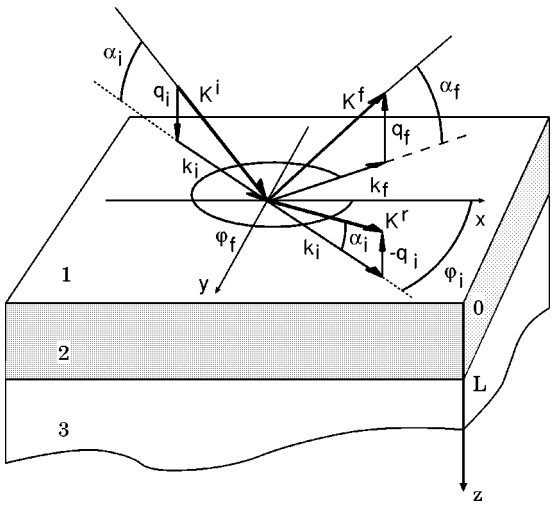

FIG. 10. A film ($0<z<L$) filled with material 2 is sandwiched in between a half-space $z<0$ filled with material 1 (typically vacuum) and a half-space $z>L$ filled with material 3 acting as a supporting substrate for the film. A plane wave with wave vector $\mathbf{K}^i=(\mathbf{k}_i,q_i)=K^i(\cos\alpha_i\cos\varphi_i,\cos\alpha_i\sin\varphi_i,\sin\alpha_i)$ impinges on the 1-2 interface at $z=0$. The reflected beam has the wave vector $\mathbf{K}^r=(\mathbf{k}_i,-q_i)$; the transmitted beam is not shown. Fluctuations in the film give rise to an off specular elastic diffuse scattering with $\mathbf{K}^f=(\mathbf{k}_f,q_f)=K^f(\cos\alpha_f\cos\varphi_f,\cos\alpha_f\sin\varphi_f,-\sin\alpha_f)$, $K^f=K^i=K$.

ignored. Within the plane of incidence there is a specularly reflected wave with $\mathbf{K}^r=(\mathbf{k}_i,-q_i)$. The mean value of the electron density in the case of x rays and of the scattering length in the case of neutrons determine the intensity of the reflected beam whereas fluctuations around the mean value give rise to scattered intensity in off-specular directions $\mathbf{K}^f=(\mathbf{k}_f,q_f<0)$ with $q_f=-K^f\sin\alpha_f$ and $\mathbf{k}_f=K^f\cos\alpha_f(\cos\varphi_f,\sin\varphi_f,0)$. We consider only elastic scattering, i.e., $K^i=K^f=K^r\equiv K$. (For the more complex case of neutron scattering under grazing incidence from magnetic systems, see Ref. 83.)

In order to proceed, we assume that the mean values of the electron density or of the scattering length density in each medium is constant and varies steplike across the two interfaces 1-2 and 2-3. This gives rise to the following indices of refraction:[50]

$$z<0: n=n_1=1, \quad 0<z<L: n=n_2=1-\delta_2+i\beta_2, \qquad z>L: n=n_3=1-\delta_3+i\beta_3. \tag{4.1}$$

In Eqs. (4.1) we consider the case that medium 1 is vacuum and the generic case for hard x rays that Re $n<1$ in condensed matter. Although for neutrons one can also have Re $n>1$, in order to limit the number of possible relative values of the indices of refraction for the materials 1, 2, and 3 we do not analyze this latter case in more detail. For x rays $\delta=\lambda^2(r_e/2\pi)\Sigma_i N_i Z_i$ and the extinction coefficient $\beta=(\lambda/4\pi)\Sigma_i N_i\sigma_{a,i}\equiv\lambda\mu_{abs}/4\pi$, where $r_e=e^2/4\pi\epsilon_0 mc^2=2.814\times10^{-5}$ Å is the classical electron radius, and N_i the number density of atoms of species i with Z_i electrons and absorption cross section $\sigma_{a,i}$. For neutrons $\delta=(\lambda^2/2\pi)\Sigma_i N_i b_i$ and $\beta=(\lambda/4\pi)\Sigma_i N_i\sigma_{t,i}$ where b_i is the nuclear scattering length of species i. $\sigma_{t,i}$ is the cross section taking into account incoherent scattering and nuclear reactions. Typically δ and β are of the order 10^{-5}. For Re $n<1$, total external reflection occurs for $\alpha<\alpha_c$. For $L=\infty$ one has $\alpha_{c12}\simeq(2\delta_2)^{1/2}$, whereas for $L=0$ $\alpha_{c13}\simeq(2\delta_3)^{1/2}$. Since the angle of total reflection depends only on the difference $n(z\to-\infty)-n(z\to+\infty)>0$, for any finite $0<L<\infty$ the incoming wave is totally reflected for $\alpha<\alpha_{c13}$, independent of the index of refraction within the film. Nonetheless the types of waves propagating in the film depend on whether $\alpha\gtrless\alpha_{c12}$ (see below). For the present setup the wave field has the form $\Psi(\mathbf{r},\mathbf{K}^i)=e^{i\mathbf{k}_i\cdot\mathbf{r}_\parallel}\psi(z,\alpha)$ with

$$\psi(z,\alpha)=\begin{cases} e^{iq_1(\alpha)z}+r_L(\alpha)e^{-iq_1(\alpha)z}, & z<0 \\ s_+(\alpha)e^{iq_2(\alpha)z}+s_-(\alpha)e^{-iq_2(\alpha)z}, & 0\leqslant z\leqslant L \\ t_L(\alpha)e^{iq_3(\alpha)z}, & z>L, \end{cases} \tag{4.2}$$

where

$$\begin{aligned} r_L(\alpha)&=[(q_1-q_2)(q_2+q_3)+e^{2iq_2L}(q_1+q_2)(q_2-q_3)]/\Lambda(\alpha), \\ s_+(\alpha)&=2q_1(q_2+q_3)/\Lambda(\alpha), \\ s_-(\alpha)&=2q_1(q_2-q_3)e^{2iq_2L}/\Lambda(\alpha), \\ t_L(\alpha)&=4q_1q_2e^{i(q_2-q_3)L}/\Lambda(\alpha), \\ \Lambda(\alpha)&=(q_1+q_2)(q_2+q_3)+e^{2iq_2L}(q_1-q_2)(q_2-q_3). \end{aligned} \tag{4.3}$$

Since the scattering cross section is independent of the intensity of the incoming beam without loss of generality, we have set the amplitude of $\Psi(\mathbf{r},\mathbf{K}^i)$ equal to 1. The vertical components of the momentum are given by

$$\begin{aligned} q_1(\alpha)&=K\sin\alpha, \\ q_j(\alpha)&=K\sqrt{n_j^2-\cos^2\alpha}\simeq K\sqrt{\sin^2\alpha-2\delta_j+2i\beta_j} \\ &=K\sqrt{\sin^2\alpha-\sin^2\alpha_{c1j}+2i\beta_j}, \quad j=2,3. \end{aligned} \tag{4.4}$$

In the limiting case that the film turns into a semi-infinite substrate, i.e., $L=\infty$, one has

$$\psi_{\infty/2}(z,\alpha)=\begin{cases} e^{iq_1(\alpha)z}+r_{\infty/2}(\alpha)e^{-iq_1(\alpha)z}, & z<0 \\ t_{\infty/2}(\alpha)e^{iq_2(\alpha)z}, & z\geqslant 0, \end{cases} \tag{4.5}$$

with

$$r_{\infty/2}(\alpha)=(q_1-q_2)/(q_1+q_2), \quad t_{\infty/2}(\alpha)=2q_1/(q_1+q_2). \tag{4.6}$$

The vertical momentum components $q_j(\alpha)$ have a positive imaginary part which is due to the extinction coefficient β_j for $\alpha>\alpha_{c1j}$ and which is present for $\alpha<\alpha_{c1j}$ even in the absence of absorption. This gives rise to an exponentially damped evanescent wave with a penetration depth $l_j=[\mathrm{Im}\, q_j(\alpha)]^{-1}$ which increases steeply for $\alpha\nearrow\alpha_{c1j}$ and would diverge if $\beta_j=0$. Within the film there is a superposition of two fields $s_+(\alpha)e^{iq_2(\alpha)z}$ and $s_-(\alpha)e^{-iq_2(\alpha)z}$ [Eq. (4.2)]; in the three cases $\alpha<\alpha_{c12}$ and $\beta_2=0$, $\alpha>\alpha_{c12}$ and $\beta_2\neq0$, and $\alpha<\alpha_{c12}$ and $\beta_2\neq0$, $q_2(\alpha)$ has a nonzero imaginary part leading to an exponentially increasing and decreasing contribution for increasing z. The decreasing part corre-

sponds to the damping of the incident wave, whereas the increasing part corresponds to the damping of the reflected wave generated by the interface 2-3.

Equation (4.2) describes the wave field $\Psi(\mathbf{r},\mathbf{K}^i)$ in the absence of any fluctuations. This wave field is scattered at the fluctuating inhomogeneities within the film giving rise to diffuse scattering intensities in off-specular directions.

The computation of this intensity requires one to specify the nature of fluctuations. In the present context this amounts to specifying the kind of system undergoing the continuous phase transition in the film, and choosing the appropriate order parameter. As described in Sec. I, the most promising candidates for these kinds of phenomena are binary alloys undergoing a continuous order-disorder phase transition concerning the occupation of fixed lattice sites $\{\mathbf{R}_l\}$. (Magnetic films are equally well suited. However, the magnetic scattering of neutrons[83] or of x rays is more complicated, and requires separate analyses. Although the details will differ from the analysis given below, the key features of the singularities are expected to be borne out similarly.) In these systems a given configuration is characterized by spin-type variables $\{S_l=\pm 1\}$ such that $S_l=+1$ (-1) states that the lattice site $\mathbf{R}_l$ is occupied by a B (A) atom. Accordingly the number density of electrons for such a configuration is

$$\rho(\mathbf{r})=\frac{1}{2}\sum_l \{\rho_B(\mathbf{r}-\mathbf{R}_l)+\rho_A(\mathbf{r}-\mathbf{R}_l) + S_l[\rho_B(\mathbf{r}-\mathbf{R}_l)-\rho_A(\mathbf{r}-\mathbf{R}_l)]\}, \tag{4.7}$$

where $\rho_{A(B)}(\mathbf{r})$ is the electron number density in a single unit cell V_{cell} occupied by an $A(B)$ atom. [In the case of neutron scattering, $\rho(\mathbf{r})$ stands for the scattering length density and $\rho_{A(B)}(\mathbf{r})=b_{A(B)}\delta(\mathbf{r})$, where $b_{A(B)}$ is the mean scattering length of the nuclei of species $A(B)$.] The ordered state of this system corresponds to a configuration in which the sign of S_l alternates from one lattice site to any of the neighboring ones. In this ground state the staggered ''magnetization'' $OP_l=S_l e^{i\boldsymbol{\tau}_m\cdot\mathbf{R}_l}$ is spatially constant if the reciprocal lattice vector $\boldsymbol{\tau}_m$ of the sublattice structure is chosen such that $e^{i\boldsymbol{\tau}_m\cdot(\mathbf{R}_l-\mathbf{R}_{l'})}=-1$ for nearest-neighbor sites $\mathbf{R}_l$ and $\mathbf{R}_{l'}$. In reciprocal space the positions of the reciprocal sublattice vectors $\boldsymbol{\tau}_m$ are halfway in between the reciprocal-lattice vectors $\mathbf{G}_m$, with $e^{i\mathbf{G}_m\cdot\mathbf{R}_l}$ characterizing the underlying lattice structure of the solid. (For the sake of simplicity, as far as the scattering theory is concerned, here we do not explicitly consider the case of systems like Fe_3Al whose description requires the introduction of several sublattices.) Upon approaching the critical temperature of the continuous order-disorder transition, the thermal average $\langle OP_l\rangle$ vanishes, qualifying OP_l as an appropriate order parameter.

In the critical contribution to the *bulk* scattering cross section a nonzero value of $\langle OP_l\rangle$ leads to superlattice Bragg peaks:[49]

$$\left(\frac{d\sigma}{d\Omega}\right)_{bulk}^{Bragg}=r_e^2\left(\frac{\mathbf{K}^f}{K}\times\mathbf{e}\right)^2\langle OP_l\rangle^2\frac{N_V}{V_{cell}}(2\pi)^3 \times\sum_m |\tilde{F}e^{-W}|^2\delta(\mathbf{K}^i-\mathbf{K}^f-\boldsymbol{\tau}_m), \tag{4.8}$$

where r_e is the classical electron radius, $\mathbf{K}^f/K$ are the directions of observation, $\mathbf{e}$ is the polarization vector of the incoming electromagnetic wave, and $\tilde{F}=(F_A-F_B)/2$, where $F_{A(B)}(\mathbf{K})=\int_{V_{cell}}d^3r\rho_{A(B)}(r)e^{i\mathbf{K}\cdot\mathbf{r}}$ is the atomic form factor of the atom $A(B)$, $e^{-W(\mathbf{K})}$ is the Debye-Waller factor, and N_V is the number of lattice sites in the sample. With the independent knowledge of all prefactors in Eq. (4.8) the asymptotic temperature dependence of $(d\sigma/d\Omega)_{bulk}^{Bragg}$ yields $\langle OP_l\rangle=\mathcal{B}'(-t)^\beta$. As discussed in Sec. II, this experimental value for $\mathcal{B}'$ enters into Eq. (2.21) and there replaces B if $G(p,z_1,z_2,L,t)$ corresponds to the pair correlation function $\langle OP_lOP_{l'}\rangle$ as considered below. Similarly the singular diffuse scattering around a superlattice Bragg peak $\boldsymbol{\tau}_m$ is given by

$$\left(\frac{d\sigma}{d\Omega}\right)_{bulk}^{diffuse}=r_e^2\left(\frac{\mathbf{K}^f}{K}\times\mathbf{e}\right)^2|\tilde{F}e^{-W}|^2\sum_{\mathbf{R}_l,\mathbf{R}_{l'}}(\langle OP_lOP_{l'}\rangle -\langle OP_l\rangle\langle OP_{l'}\rangle)e^{i\mathbf{q}\cdot(\mathbf{R}_l-\mathbf{R}_{l'})} \rightarrow r_e^2\left(\frac{\mathbf{K}^f}{K}\times\mathbf{e}\right)^2|\tilde{F}e^{-W}|^2\frac{N_V}{V_{cell}}G_{bulk}(\mathbf{q},t), \tag{4.9}$$

with $\mathbf{q}=\mathbf{K}^f-\mathbf{K}^i-\boldsymbol{\tau}_m$. In the second part of Eq. (4.9) we have performed the continuum limit, replacing the lattice sums by integrals [see Eq. (A3) and the last paragraph in Sec. II], because for $\xi\rightarrow\infty$ the lattice structure becomes irrelevant. From studying the temperature dependence of Eq. (4.9) for $T>T_c$, one can infer the correlation length ξ and its amplitude ξ_0^+ introduced in Sec. II. We note that for q small compared with the inverse lattice spacing a, Eqs. (A3) and (A5) can be applied to Eq. (4.9) provided B is replaced by $\mathcal{B}'$ as determined from Eq. (4.8).

Equipped with this knowledge about the critical bulk scattering (i.e., above the angle of total reflection and for a bulk sample), we can now turn to the critical diffuse scattering from the film. Within the so-called distorted wave Born approximation and for the model of the film as described above one finds the following expressions for the singular part of the coherent scattering cross section:[49]

$$\frac{d\sigma}{d\Omega}=r_e^2\frac{A_\parallel}{(V_{cell}^\parallel a)^2}|\tilde{F}e^{-W}|^2\Sigma, \tag{4.10}$$

$$\Sigma=\int_0^L dz_1\int_0^L dz_2\psi_f(z_1)\psi_i(z_1)\psi_i^*(z_2)\psi_f^*(z_2) \times G(p,z_1,z_2,L,t),$$

where $A_\parallel=N_\parallel V_{cell}^\parallel$ is the illuminated surface area, where $N_\parallel$ is the number of lattice sites at the surface and $V_{cell}^\parallel$ is the two-dimensional unit cell of the surface, a is the lattice spacing of the cubic lattice, $\psi_{i,f}(z)\equiv\psi(z,\alpha=\alpha_{i,f})$ [see Eq. (4.2) and Fig. 10], and $\mathbf{p}=\mathbf{k}^f-\mathbf{k}^i-\boldsymbol{\tau}_m$ assuming that the film surfaces are cut such that $\boldsymbol{\tau}_m$ is parallel to them. G is the lateral Fourier transform of the two-point order parameter correlation function

$$G(p,z_1,z_2,L,t)=\frac{V_{cell}^{\|}}{N_{\|}}\sum_{\mathbf{r}_{\|}^{(m)},\mathbf{r}_{\|}^{(m')}} e^{i\mathbf{p}\cdot(\mathbf{r}_{\|}^{(m)}-\mathbf{r}_{\|}^{(m')})} \times[\langle OP(\mathbf{r}_{\|}^{(m)},z_1)OP(\mathbf{r}_{\|}^{(m')},z_2)\rangle - \langle OP(\mathbf{r}_{\|}^{(m)},z_1)\rangle\langle OP(\mathbf{r}_{\|}^{(m')},z_2)\rangle] \rightarrow \int d^2r_{\|}e^{-i\mathbf{p}\cdot\mathbf{r}_{\|}}G(\mathbf{r}_{\|},z_1,z_2,L,t) \quad (4.11)$$

on the lattice and in the continuum limit, respectively. Thus after replacing the nonuniversal amplitude B in Eq. (2.21) by $\mathcal{B}'$ as obtained from Eq. (4.8) for $\langle OP_l\rangle$, we can study the scattering cross section in Eq. (4.10) by using all the information about $G(p,z_1,z_2,L,t)$ obtained in Sec. III, provided all lengths and $1/p$ are sufficiently large compared with the lattice spacing a so that the continuum description is applicable.

In view of the properties of the wave functions ψ (only their functional forms for $0\leqslant z\leqslant L$ enter into Σ [see Eq. (4.2)] and of the scaling form for $G(p,z_1,z_2,L,t)$ [see Eq. (2.21)]), one has, for $\alpha_{i,f},\alpha_{c12,c13}\ll 1$ and $\beta_{2,3}=0$,

$$\Sigma=\mathcal{B}'(\xi_0^+)^{d+1}\mathcal{R}\left(\frac{L}{\xi_0^+}\right)^{3-\eta}\sigma\left(p\xi,\frac{L}{\xi},\frac{l_i}{L},\frac{l_f}{L},\frac{\alpha_i}{\alpha_{c12}},\frac{\alpha_{c12}}{\alpha_{c13}}\right), \quad (4.12)$$

where the dimensionless function σ is given by [Eq. (2.21)]

$$\sigma=\int_0^1 dx_1\int_0^1 dx_2\psi_f(z_1=x_1L)\psi_i(z_1=x_1L) \times\psi_i^*(z_2=x_2L)\psi_f^*(z_2=x_2L)x_1^{1-\eta} \times g_{\mathrm{II}}\left(pLx_2,\frac{L}{\xi}x_1,\frac{L}{\xi}x_2,x_2\right). \quad (4.13)$$

The two variables $p\xi$ and L/ξ of σ stem from the scaling function, of the pair correlation function whereas the dependences of σ on l_i/L, l_f/L, α_i/α_{c12}, and $\alpha_{c12}/\alpha_{c13}$ are due to the wave functions. For $\alpha_{i,f}<\alpha_{c12}$,

$$l_{i,f}=\frac{l_0^{(2)}}{\sqrt{1-\left(\frac{\alpha_{i,f}}{\alpha_{c12}}\right)^2}} \quad (4.14)$$

correspond to the *penetration depths of* the incoming (i) and outgoing (f) evanescent wave, respectively, *within the film material 2*. $l_0^{(2)}=(K\alpha_{c12})^{-1}$ is the minimal penetration depth $l_{i,f}(\alpha_{i,f}=0)$ in the film material. Typically l_0 is of the order of 30 Å.[50] For $\alpha_i>\alpha_{c12}$ and $\alpha_f>\alpha_{c12}$ the corresponding quantities l_i and l_f, respectively, are purely imaginary.

B. Interplay of length scales

The scattering cross section reflects the rich interplay of five length scales: $1/p$, ξ, l_i, l_f, and L. Scaling reduces that to four independent scaling variables; moreover, there is a parametric dependence on α_i/α_{c12} and on the material constant $\alpha_{c12}/\alpha_{c13}$. It is beyond the scope of the present analysis to provide an exhaustive discussion of the full dependence on all these variables. Instead we discuss some general aspects and analyze a few specific cases in more detail in order to highlight the key features of the diffuse scattering intensity. The following cases have to be distinguished (for $T\geqslant T_c$).

(Ia) $l_{i,f}\ll L$ and total reflection at 2-3 interface: $d\sigma/d\Omega$ is proportional to the scattering volume $A_{\|}\min(l_i,l_f)$. (1) $\xi\ll l_{i,f}\ll L$: bulk behavior convoluted with evanescent waves. (2) $\xi\sim l_{i,f}\ll L$: crossover bulk-$\infty/2$ surface behavior convoluted with evanescent waves. (3) $l_{i,f}\ll\xi\ll L$: $\infty/2$ surface behavior convoluted with evanescent waves. (4) $l_{i,f}\ll\xi\sim L$: $\infty/2$ surface behavior plus distant wall correction convoluted with evanescent waves. (5) $l_{i,f}\ll L\ll\xi$: film behavior near one wall convoluted with evanescent waves.

(Ib) $l_{i,f}\ll L$, and no total reflection at 2-3 interface: the difference from case (Ia) is exponentially small, i.e., $\sim e^{-LK}$. (The volume contribution to $d\sigma/d\Omega$ from material 3 is insignificant because it does not exhibit critical fluctuations.)

(IIa) $l_{i,f}\sim L$, and total reflection at 2-3 interface: crossover between $d\sigma/d\Omega\sim A_{\|}\min(l_i,l_f)$ to $d\sigma/d\Omega\sim A_{\|}L$. (1) $\xi\ll l_{i,f}\sim L$: $\infty/2$ surface behavior convoluted with film wave functions. (2) $\xi\sim l_{i,f}\sim L$: crossover bulk-$\infty/2$ surface behavior convoluted with film wave functions. (3) $l_{i,f}\sim L\ll\xi\rightarrow\infty$: film behavior convoluted with film wave functions.

(IIb) $l_{i,f}\sim L$, and no total reflection at 2-3 interface: crossover $d\sigma/d\Omega\sim A_{\|}\min(l_i,l_f)\rightarrow A_{\|}L$. (Again, the volume contribution from material 3 is regarded to be insignificant and is not taken into account.)

(IIIa) $l_{i,f}\gg L$, and total reflection at 2-3 interface: $d\sigma/d\Omega\sim A_{\|}L$. (1) $\xi\ll L\ll l_{i,f}$: bulk behavior convoluted with film wave functions. (2) $\xi\sim L\ll l_{i,f}$: crossover between bulk and film behavior (including two surface contributions and distant wall corrections) convoluted with film wave functions. (3) $L\ll\xi\ll l_{i,f}$: film behavior convoluted with film wave functions. (4) $L\ll\xi\sim l_{i,f}$: film behavior convoluted with film wave functions. (5) $L\ll l_{i,f}\ll\xi\rightarrow\infty$: film behavior convoluted with film wave functions.

(IIIb) $l_{i,f}\gg L$, and no total reflection at 2-3 interface: $d\sigma/d\Omega\sim A_{\|}L$. (The volume contribution from material 3 is regarded to be insignificant.)

(IVa) $l_{i,f}$ imaginary, and total reflection at 2-3 interface: $d\sigma/d\Omega\sim A_{\|}L$. (1) $\xi\ll L$: three-dimensional bulk behavior probed by undistorted plane waves. (2) $L\ll\xi$: film behavior probed by undistorted plane waves.

(IVb) $l_{i,f}$ imaginary, and no total reflection at 2-3 interface: $d\sigma/d\Omega\sim A_{\|}L$ (in addition to an insignificant volume contribution from material 3).

C. Susceptibility from the scattering cross section

For large penetration depths $l_{i,f}\gg L$, the product of wave fields in Eq. (4.13) is approximately constant. In this case for $p=0$ the universal scaling function σ of Eq. (4.13) reduces up to a prefactor to the scaling function f of the total susceptibility [see Eqs. (3.24) and (3.25)], i.e.,

$$\sigma\left(\frac{L}{\xi}\right)=\sigma\left(p\xi=0,\frac{L}{\xi},\frac{l_i}{L}=\infty,\frac{l_f}{L}=\infty,\frac{\alpha_i}{\alpha_{c12}}<1,\frac{\alpha_{c12}}{\alpha_{c13}}\right)\sim f\left(\frac{L}{\xi}\right). \quad (4.15)$$

In this limit the dependences on α_i/α_{c12} and on $\alpha_{c12}/\alpha_{c13}$ drop out for $\alpha_i<\alpha_{c13}$; for $\alpha_i>\alpha_{c13}$ there is an insignificant

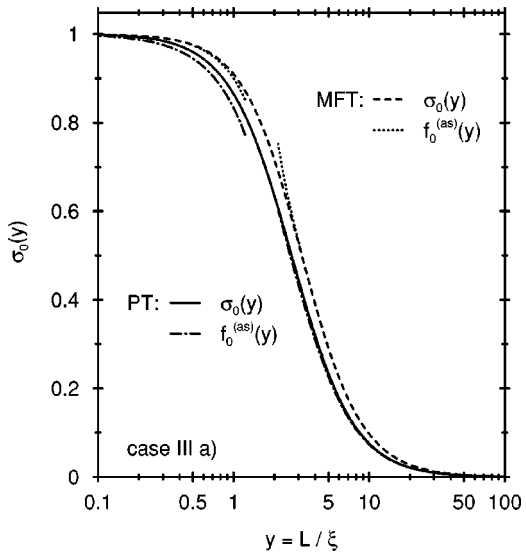

FIG. 11. Scaling function of the scattering cross section σ [Eq. (4.13)] for large penetration depths $l_{i,f} \gg L$ and vanishing lateral momentum $p=0$ as a function of the scaling variable $y=L/\xi$ within MFT (dashed line) and perturbation theory (full line). The dotted and dashed-dotted lines correspond to the asymptotic behaviors $f_0^{(as)}(y)$ of the normalized scaling function $f_0(y)=f(y)/f(0)$ of the total susceptibility $f(y)$ [Eqs. (3.26) and (3.40)] in MFT and PT to first order in ϵ using in addition the best available exponents, respectively.

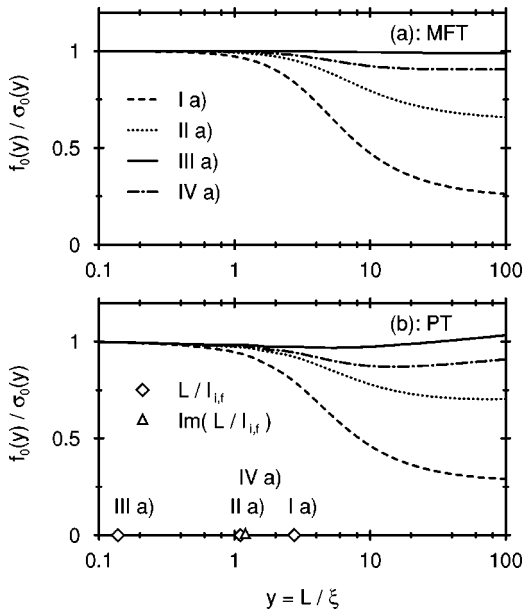

FIG. 12. Ratio of the normalized scaling functions of the total susceptibility [Eq. (3.24)] and of the scattering cross section [Eq. (4.13)] within MFT (a) and PT (b). We use the normalization $\sigma_0(y)=\sigma(y)/\sigma(0)$ and $f_0(y)=f(y)/f(0)$. The various lines in (a) and (b) correspond to different penetration depths $l_{i,f}$: (Ia) $l_{i,f} \ll L$, (IIa) $l_{i,f} \sim L$, (IIIa) $l_{i,f} \gg L$, and (IVa) $l_{i,f}$ imaginary (no total reflection at the interface 1-2) as marked in (b). The curves correspond to $l_i = l_f$. In case (IVa), the indicated value of $L/l_{i,f}$ corresponds to its imaginary part.

bulk contribution from material 3. The five different cases (1)–(5) in case (IIIa) are characterized by the various contributions of asymptotic behaviors to the scaling function $\sigma(y=L/\xi) \sim f(y)$ [see Eqs. (3.26) and (3.40)], i.e., bulk $\mathcal{A}y^{-2+\eta}$, surface $\mathcal{B}y^{-3+\eta}$, distant wall $\mathcal{C}y^{-3+\eta}e^{-y}$, and film behavior $\mathcal{D}+\mathcal{E}y^{1/\nu}$. In Fig. 11 we show the normalized scaling function of the scattering cross section $\sigma_0(y)=\sigma(y)/\sigma(0)$ [Eq. (4.13)] within mean-field and first-order perturbation theory, as well as the asymptotic behaviors of the normalized scaling function $f_0(y)=f(y)/f(0)$ of the total susceptibility $f(y \to 0)$ [Eq. (3.40)] and $f(y \to \infty)$ [Eq. (3.26)] using mean-field exponents and amplitudes and best values for the exponents and amplitudes to first order in ϵ, respectively. Cases (IIIa) or (IIIb) with lateral momentum $p=0$ are the appropriate scattering setups in order to measure the various asymptotic behaviors of the total susceptibility by varying the temperature.

Figure 12 shows the ratio of the normalized scaling functions $f_0(y)/\sigma_0(y)=[f(y)/\sigma(y)][\sigma(0)/f(0)]$ for all four cases (Ia) – (IVa) within MFT and PT, respectively. For large penetration depths $l_{i,f} \gg L$ [see case (IIIa)] the deviation of the scaling function $\sigma_0(y)$ of the scattering cross section from the scaling function $f_0(y)$ of the total susceptibility is small [see the solid lines in Figs. 12(a) and 12(b)]. If the penetration depths are of the order of the film thickness, $l_{i,f} \sim L$ [see case (IIa)], the wave fields in Eq. (4.13) contribute, and the deviation from the total susceptibility becomes visible at large values of the scaling variable y. For $y \to 0$ and $y \to \infty$ the dotted lines attain constant values, so that there are the same critical exponents but different amplitudes for the leading asymptotic behaviors of σ_0 and f_0. If the penetration depths are smaller than the film thickness, $l_{i,f} \ll L$ [see case (Ia)], this deviation is much more pronounced (see dashed lines). The difference in the amplitudes is decreased if $\alpha_{i,f} > \alpha_{c12}$, i.e., for imaginary $l_{i,f}$ [see case (IVa), and dash-dotted lines].

D. Dependence on the film thickness

In order to reveal the $(1/L)^{-1+\eta_\parallel}$ cusp singularity in the scattering cross section, we consider the case $p=t=0$ and introduce the corresponding scattering function

$$\Sigma_L = \int_0^L dz_1 \int_0^L dz_2 \psi_f(z_1)\psi_i(z_1)\psi_i^*(z_2)\psi_f^*(z_2) \times G(p=0,z_1,z_2,L,t=0), \tag{4.16}$$

where the wave fields are given in Eq. (4.2). For the correlation function G we use the asymptotic expansion given by Eq. (3.21). Furthermore we introduce the scattering function of the semi-infinite system

$$\Sigma_{\infty/2} = \int_0^\infty dz_1 \int_0^\infty dz_2 \psi_{\infty/2}^{(f)}(z_1)\psi_{\infty/2}^{(i)}(z_1)\psi_{\infty/2}^{(i)*}(z_2)\psi_{\infty/2}^{(f)*}(z_2) \times G(p=0,z_1,z_2,L=\infty,t=0), \tag{4.17}$$

with the wave fields and the correlation function given in Eqs. (4.5) and (3.18), respectively. The ratio of Eqs. (4.16) and (4.17) defines the scattering function

$$S(LK;\alpha_i,\alpha_f,\alpha_{c12},\alpha_{c13},\beta_2,\beta_3) = \frac{\Sigma_L}{\Sigma_{\infty/2}} \tag{4.18}$$

for $p=t=0$, where the film thickness L and the momentum K of the scattered wave form the scaling variable, the angles $\alpha=\{\alpha_{i,f},\alpha_{c12,c13}\}$ characterize the scattering geometry, and the extinction coefficients $\beta=\{\beta_2,\beta_3\}$ take into account photo absorption. From Eqs. (C3)–(C8) in Appendix C, one obtains the asymptotic expansion

$$S(LK\to\infty;\alpha,\beta)=s_0(LK;\alpha,\beta)+s_1(LK;\alpha,\beta)C_1\left(\frac{1}{LK}\right)^{-1+\eta_\parallel}+\cdots, \tag{4.19}$$

with

$$s_0(LK\to\infty;\alpha,\beta)\sim 1+s_0^{(1)}(LK;\alpha,\beta)e^{-LKs_0^{(2)}(\alpha,\beta)}, \tag{4.20}$$

$$s_1(LK\to\infty;\alpha,\beta)\sim s_1^{(0)}(LK=\infty;\alpha,\beta)+s_1^{(1)}(LK;\alpha,\beta)e^{-LKs_1^{(2)}(\alpha,\beta)},$$

and C_1 given by Eq. (3.9). The functions s_0 and s_1 carry the L dependence of the wave functions (see Appendix D). The L dependence due to the correlation function is given by the cusp singularity $C_1(1/LK)^{-1+\eta_\parallel}$. The range of the values of the scaling variable $(LK)^{-1}$ is limited by the validity of the continuum theory applied here, i.e., $L\gtrsim 30$ Å and the distorted-wave Born approximation, i.e., $K\gtrsim 1$ Å^{-1}, leading to $(LK)^{-1}\lesssim\frac{1}{30}$. For small angles, i.e., for grazing incidence scattering experiments Eq. (4.4) reduces

$$q_1(\alpha)\simeq K\alpha,\quad q_j(\alpha)\simeq K\sqrt{\alpha^2-\alpha_{c1j}^2+2i\beta_j},\quad j=2,3. \tag{4.21}$$

Photoabsorption, $\beta_2\neq 0$, or evanescent scattering, $\alpha_{i,f}<\alpha_{c12}$, turn q_2 into an imaginary quantity, which leads to a real part of $s_0^{(2)}$ and $s_1^{(2)}$ in Eq. (4.20). If at least one angle α_i or α_f is larger than the critical angle α_{c12}, the functions $s_0^{(1)}$ and $s_1^{(2)}$ have real and imaginary parts. In the latter case one expects that the scattering function S in Eq. (4.19) exhibits an oscillatory behavior. In Fig. 13 we show the exponentiated scattering function and its asymptotic form for various scattering geometries. The exponentiated form is obtained by subtracting the leading behavior of the one-loop ϵ-expanded result [defined by Eq. (4.18)], and by adding the leading behavior [see Eq. (C2)] calculated with the best available critical exponents ($\eta\simeq 0.031$, $\eta_\perp\simeq 0.75$, and $\eta_\parallel\simeq 1.48$). The dashed line in Fig. 13 corresponds to the leading asymptotic behavior, if the L dependence of the wave fields is neglected:

$$S(LK\to\infty;\alpha,\beta)=1+s_1^{(0)}(LK=\infty;\alpha,\beta)C_1\left(\frac{1}{LK}\right)^{-1+\eta_\parallel}+\cdots. \tag{4.22}$$

Thus the full lines in Fig. 13 take into account the whole L dependence stemming from both the scattering theory and the correlation function, whereas the dashed lines take into account only the leading asymptotic L dependence of the correlation function. The oscillatory behavior appearing for $\alpha_i\lessgtr\alpha_{c12}\lessgtr\alpha_f$ stems from the scattering theory (see Fig. 13).

For the case $\alpha_{i,f}<\alpha_{c12,c13}$ in Fig. 13, half of the maximum value of the scattering function S is reached for $LK\simeq 1.5\times 10^{-3}$. This corresponds to a film thickness $L\simeq 600$ Å, i.e., 200 ML (with $K\simeq 1$ Å^{-1} and 1 ML is approximately 3 Å thick); 90% of the maximum value of S is reached for $LK\simeq 5\times 10^{-5}$ which corresponds to a film thickness $L\simeq 20\,000$ Å or 6700 ML. This demonstrates the slow convergence to the semi-infinite limit. The spatial resolution is determined by the uncertainty of the film thickness. With $\Delta L\simeq 3$ Å (1 ML) this gives $K\Delta L\simeq 3$ leading to a resolution of $\Delta(LK)^{-1}\sim 3/(LK)^2$, which is not visible on the scale of Fig. 13. Based on these considerations, we conclude that the oscillations are experimentally accessible.

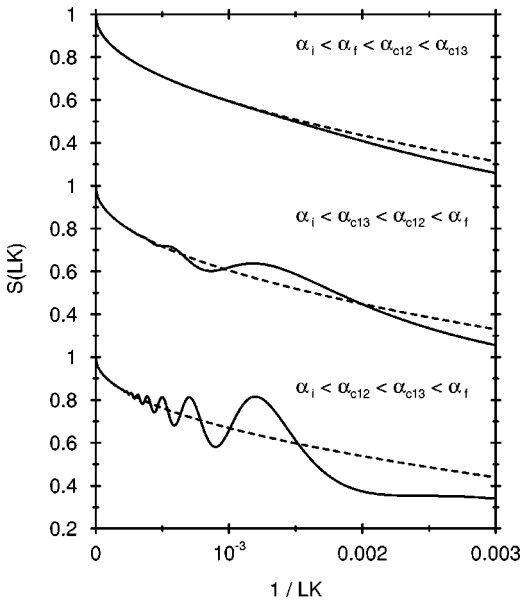

FIG. 13. Scattering function $S(LK;\alpha,\beta)$ [Eq. (4.18), full lines] and its asymptotic form $S(LK\to\infty;\alpha,\beta)$ [Eq. (4.22), dashed lines] for three different scattering geometries: $\alpha_i<\alpha_f<\alpha_{c12}<\alpha_{c13}$, $\alpha_i<\alpha_{c13}<\alpha_{c12}<\alpha_f$, and $\alpha_i<\alpha_{c12}<\alpha_{c13}<\alpha_f$. For $\alpha_{i,f}<\alpha_{c12,c13}$ the scattering function decreases monotonously. If one of the angles α_i or α_f is larger than α_{c12} oscillations emerge. This effect is enhanced if $\alpha_{c13}>\alpha_{c12}$. In the asymptotic form of Eq. (4.22) (dashed lines) there are no oscillations. In all three cases $\beta_{2,3}=0.3\times 10^{-5}$ and $(\alpha_i,\alpha_f,\alpha_{c12},\alpha_{c13}=0.06°,0.11°,0.26°,0.36°)$, (0.06°,0.40°,0.36°,0.26°), and (0.06°, 0.40°,0.26°,0.36°), respectively.

E. Emergence of cusp singularities

In the following we analyze how the cusp singularities emerge in the limit of vanishing scaling variables. To this end we chose, as an example, a scattering function of the two scaling variables p/K and LK. Analogous to Eq. (4.16), we define the quantity

$$\Sigma_{p,L}=\int_0^L dz_1\int_0^L dz_2\,\psi_f(z_1)\,\psi_i(z_1)\,\psi_i^*(z_2)\,\psi_f^*(z_2)\times G(p,z_1,z_2,L,t=0). \tag{4.23}$$

Together with Eq. (4.17), this leads to the scattering function

$$S(p/K,LK;\alpha,\beta)=\frac{\Sigma_{p,L}}{\Sigma_{\infty/2}} \tag{4.24}$$

where $\alpha=\{\alpha_{i,f},\alpha_{c12,c13}\}$ denotes the set of angles, and $\beta=\{\beta_{2,3}\}$ the extinction coefficients. As in Sec. III A and Eq. (3.13), we introduce polar coordinates

$$\omega=\sqrt{(p/K)^2+(LK)^{-2}},\quad \varphi=\arctan(pL),$$
$$(LK)^{-1}=\omega\cos\varphi,\quad p/K=\omega\sin\varphi. \tag{4.25}$$

This leads to the relation

$$S(p/K,LK;\alpha,\beta)=S[\omega\sin\varphi,(\omega\cos\varphi)^{-1};\alpha,\beta]$$
$$=S_{polar}(\omega,\varphi;\alpha,\beta), \tag{4.26}$$

so that the leading asymptotic behavior is given by

$$S_{polar}(\omega\to 0,\varphi;\alpha,\beta)=S_0(\varphi;\alpha,\beta)+S_1(\varphi;\alpha,\beta)\omega^{-1+\eta_\parallel}+\cdots, \tag{4.27}$$

with $S_0(\varphi;\alpha,\beta)=1$. The amplitude S_1 of the leading asymptotic behavior $\omega^{-1+\eta_\parallel}$ depends not only on the polar variable φ, as it is the case for the corresponding correlation function (see Sec. III A), but also on the parameters α and β characterizing the scattering process. Within mean-field theory this amplitude is defined in Appendix C 2 by Eq. (C19). In Fig. 14(a) we show the exponentiated scattering function $S(p/K,LK;\alpha,\beta)$ [Eq. (4.24)], where we have subtracted the leading asymptotic behavior from the mean-field expression of the scattering function and added the exponentiated form, [see Eqs. (C11) and (C19) in Appendix C 2]; the scattering function S [Eq. (4.24)] is a sum [see Eq. (D1) in Appendix D] of functions of the type $\mathcal{S}$ as discussed in Eq. (C11) in Appendix C 2. Figure 14(b) illustrates the emergence of the $(p/K)^{-1+\eta_\parallel}$ cusp for increasing film thickness, i.e., $(LK)^{-1}\to 0$. Figure 14(c) shows the emergence of the $[1/(LK)]^{-1+\eta_\parallel}$ cusp for vanishing lateral momentum $p/K\to 0$. In the latter case the vertical cross sections of the manifold are not monotonous; they exhibit a maximum (●) at $1/L\neq 0$. Figure 14 corresponds to scattering angles $\alpha_{i,f}<\alpha_{c12,c13}$ which yields a monotonous behavior of the scattering function. Analogous considerations describe the emergence of the cusp singularities in the ξ-L and ξ-p dependences (see Appendix C 2).

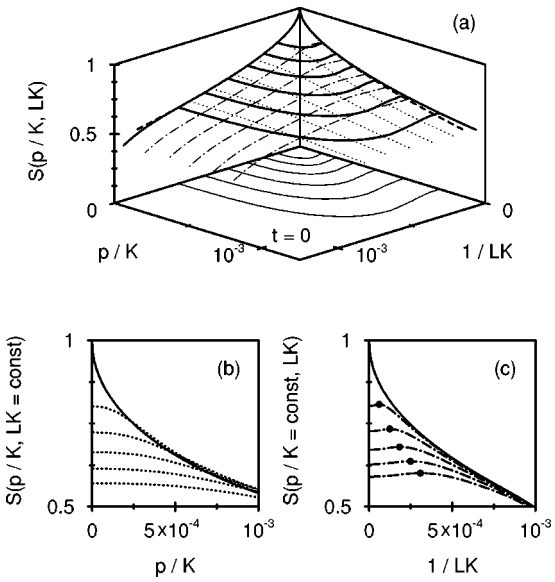

FIG. 14. Scattering function $S(p/K,LK;\alpha_{i,f},\alpha_{c12,c13},\beta_{2,3})$ [Eq. (4.24)] for $t=0$. (a) shows the exponentiated scaling functions $S(p/K,LK=\infty;\alpha,\beta)$ [Eq. (C13)] and $S(p/K=0,LK;\alpha,\beta)$ [Eq. (C14)] and their corresponding leading asymptotic behaviors [Eqs. (C15) and (C17), respectively] (dashed lines). For the leading asymptotic behavior we use the best available exponent $\eta_\parallel\simeq 1.48$ and an amplitude function which is consistent with the mean-field expression [see Eq. (C19)]. The corrections to the leading asymptotic behavior are calculated within mean-field theory. For the scaling function $S(p/K,LK;\alpha,\beta)$ we plot contour lines ($S=0.8$, 0.75, 0.7, 0.65, 0.65, and 0.6) and their projections onto the $[p/K,1/(LK)]$ plane (full lines) which clearly deviate from circular shapes, lines for $S(p/K,LK=1.5\times10^{-4}$, 3×10^{-4}, 4.5×10^{-4}, 6×10^{-4}, $7.5\times10^{-4};\alpha,\beta)$ (dotted lines) and $S(p/K=1.5\times10^{-4}$, 3×10^{-4}, 4.5×10^{-4}, 6×10^{-4}, 7.5×10^{-4}, $LK;\alpha,\beta)$ (dash-dotted lines). In (b) and (c) we show the aforementioned vertical cross sections. The emergence of the $[1/(LK)]^{-1+\eta_\parallel}$ cusp is not monotonous; the vertical cross sections exhibit maxima (●) at $1/L\neq 0$. The scattering parameters are chosen that $\alpha_i<\alpha_f<\alpha_{c12}<\alpha_{c13}$ with $(\alpha_i,\alpha_f,\alpha_{c12},\alpha_{c13})=(0.06°,0.11°,0.26°,0.36°)$ and $\beta_2=\beta_3=0.3\times10^{-5}$.

V. SUMMARY

By using field-theoretic renormalization-group theory, we have studied the singular part of the two-point correlation function in a film of thickness L near the critical point T_c of the corresponding bulk system. For $T\geqslant T_c$ and Dirichlet boundary conditions, we have obtained the following main results.

(1) The two-point correlation function as a function of the lateral momentum $\mathbf{p}$ corresponding to the $d-1$ translationally invariant directions of the film geometry, the coordinates z_1 and z_2 perpendicular to the parallel surfaces, the film thickness L, and temperature $t=(T-T_c)/T_c$ (or equivalently the bulk correlation length $\xi=\xi_0^+t^{-\nu}$) exhibits three cusp singularities: $p^{-1+\eta_\parallel}$ for $t=0$ and $L=\infty$, $(1/\xi)^{-1+\eta_\parallel}$ for $p=0$ and $L=\infty$, and $(1/L)^{-1+\eta_\parallel}$ for $p=t=0$ [see Eqs. (3.19)–(3.21) and Fig. 1]. The emergence of these three cusp singularities is revealed by studying appropriate scaling functions of two scaling variables [see Eqs. (3.10)–(3.12) and Figs. 2–8].

(2) The film correlation function calculated up to first-order perturbation theory in $\epsilon=4-d$ satisfies the so-called product rule derived by Parry and Swain for the correlation function algebra of inhomogeneous fluids in Ref. 78 [see Eq. (3.22)].

(3) By setting $p=0$ and integrating over the perpendicular coordinates z_1 and z_2, we obtain the total susceptibility of the film [Eq. (3.23)]. Its dependence on L and ξ is described by a universal scaling function $f(y=L/\xi)$ [see Eq. (3.24) and Fig. 9], and exhibits a typical film behavior: $f(y)$ is analytic for $y\to 0$ and $f(y\to\infty)$ contains the bulk, surface, and finite-size contributions [see Eqs. (3.40) and (3.26), respectively]. These properties are similar to those of the specific heat of a critical film.[30] Our results correct previous findings in the literature[68,82] [see the discussions of Eqs. (3.36) and (3.41)].

(4) In view of proposed experimental tests with x rays and neutrons under grazing incidence (see Fig. 10), as discussed in detail in Sec. I, we have calculated the critical diffuse

scattering from the film within the so-called distorted-wave Born approximation. The scattering intensity is a function of the lateral momentum transfer p, film thickness L, bulk correlation length ξ, penetration depths $l_{i,f}$ of the incoming (i) and outgoing (f) waves, the critical angles of total reflection α_{c12} and α_{c13} and the extinction coefficients β_2 and β_3 of the film (2) and the underlying substrate (3) (see Fig. 10).

(5) For various ratios of L, ξ, and $l_{i,f}$, the scattering function shows the crossover between analytic, bulk, surface, and finite-size behaviors (see Figs. 11 and 12). By varying the temperature, a scattering experiment for $p=0$ and $l_{i,f} \gg L$ gives access to the aforementioned scaling function $f(y)$ of the total susceptibility [Eq. (4.15)].

(6) For $p=t=0$ the leading singular behavior of the scattering function is given by the cusp singularity $(1/LK)^{-1+\eta_\parallel}$, where K is the momentum of the incoming wave [Eq. (4.19)]. The maximal scattering intensity for $L\to\infty$ is reached only very slowly. For certain scattering geometries the L dependence exhibits an oscillatory behavior (see Fig. 13).

(7) The film thickness and momentum cusp singularities of the correlation function are borne out in the scattering cross section, and are analyzed in Fig. 14.

ACKNOWLEDGMENTS

We thank E. Eisenriegler, A. Hanke, and M. Krech for helpful discussions. This work was supported by the German Science Foundation through Sonderforschungsbereich 237 Unordnung und große Fluktuationen.

APPENDIX A: AMPLITUDES

The amplitudes of the singular behavior of bulk correlation functions are nonuniversal. There are two independent ones in the sense that any two of them allow one to express any other in terms of these two and universal amplitude ratios.[79,80] As one of these nonuniversal amplitudes in Sec. II we have introduced and fixed the amplitude ξ_0^+ of the bulk correlation length [see Eq. (2.8)]. Other nonuniversal amplitudes are given by the temperature dependence of the mean value of the field $\phi(\mathbf{x})$ below T_c,

$$\langle \phi(\mathbf{x})\rangle = B(-t)^{\beta}, \tag{A1}$$

by the decay of the two-point correlation function in real space at T_c for large distances $|\mathbf{x}-\mathbf{x}'|$,

$$\langle \phi(\mathbf{x})\phi(\mathbf{x}')\rangle = D|\mathbf{x}-\mathbf{x}'|^{-(d-2+\eta)}, \tag{A2}$$

and in momentum space for small q,

$$\int d^d x e^{i\mathbf{q}\cdot(\mathbf{x}-\mathbf{x}')}\langle \phi(\mathbf{x})\phi(\mathbf{x}')\rangle = G_{bulk}(q,t=0) = \hat{D} q^{-2+\eta}, \tag{A3}$$

where

$$\hat{D}/D = X = 2^{2-\eta}\pi^{d/2}\frac{\Gamma(1-\eta/2)}{\Gamma[d/2-(1-\eta/2)]}. \tag{A4}$$

$\hat{D}$ can be expressed in terms of B, ξ_0^+, and a universal number R,[79,80]

$$\hat{D} = B^2(\xi_0^+)^{d-2+\eta}R, \tag{A5}$$

with $R = R_c Q_3/(R_\xi^+)^d$. For $(n,d)=(1,3)$ one has $R_c \simeq 0.066$, $Q_3 \simeq 0.922$, and $R_\xi^+ \simeq 0.27$,[79,80] leading to $R \simeq 3.09$.

A Fourier transformation in the z direction of the bulk correlation function $G_{bulk}(q) = \hat{D} q^{-2+\eta}$ with $q^2 = p^2 + k^2$ is leading to its p-z representation

$$\begin{aligned} G_{bulk}(p, z_1 - z_2) &= \int_{-\infty}^{\infty}\frac{dk}{2\pi}\hat{D}\frac{e^{ik(z_1-z_2)}}{(p^2+k^2)^{(2-\eta)/2}} \\ &= \frac{\hat{D}}{2\pi}p^{-1+\eta}\int_{-\infty}^{\infty} d\kappa \frac{e^{i\kappa p(z_1-z_2)}}{(1+\kappa^2)^{(2-\eta)/2}}. \end{aligned} \tag{A6}$$

For $p(z_1-z_2)\to 0$, this leads to

$$G_{bulk}(p) = p^{-1+\eta}\frac{\hat{D}}{2\sqrt{\pi}}\frac{\Gamma(1/2-\eta/2)}{\Gamma(1-\eta/2)}. \tag{A7}$$

In the limits $L\to\infty$, $z_1+z_2\to\infty$, $\xi\to\infty$, and $p(z_1-z_2)\to 0$, the two-point correlation function in the film reduces to its bulk form. According to Eqs. (2.12) and (2.17), this implies

$$\begin{aligned} \mathcal{G}_{\mathrm{V}} &= \frac{\hat{D}}{2\sqrt{\pi}}\frac{\Gamma(1/2-\eta/2)}{\Gamma(1-\eta/2)} \\ &= B^2(\xi_0^+)^{d-2+\eta}\frac{R}{2\sqrt{\pi}}\frac{\Gamma(1/2-\eta/2)}{\Gamma(1-\eta/2)} \\ &= B^2(\xi_0^+)^{d-2+\eta}\mathcal{U}. \end{aligned} \tag{A8}$$

For the three-dimensional Ising model, the universal number $\mathcal{U}$ has the value $\mathcal{U}\simeq 1.58$.

The knowledge of the perturbative result for $G(p,z_1,z_2,L,t)$ (see Appendix B 2) enables one to express the nonuniversal amplitudes $\mathcal{G}_x$, $x=$I–IV, in terms of $\mathcal{G}_{\mathrm{V}}$. For example the universal ratio $\mathcal{G}_{\mathrm{II}}/\mathcal{G}_{\mathrm{V}}$ is determined by the normalizations of the scaling functions, i.e., $g_{\mathrm{II}}(0,0,0,0)=1$ [Eq. (2.14)] and $g_{\mathrm{V}}(\infty,0,\infty,\infty)=1$ [Eq. (2.17)]. The ϵ expansion of this ratio is given by

$$\mathcal{G}_{\mathrm{II}}/\mathcal{G}_{\mathrm{V}} = 2\left(1+\epsilon\frac{n+2}{n+8}+O(\epsilon^2)\right). \tag{A9}$$

The amplitudes $\mathcal{G}_x$, $x=$I–IV, can have bulk, half-space, or film character, depending on the normalization limits of the scaling functions g_x. $\mathcal{G}_{\mathrm{II}}$ and $\mathcal{G}_{\mathrm{V}}$ are half-space and bulk amplitudes, respectively. Bulk amplitudes are independent of the boundary conditions, half-space amplitudes depend on the boundary condition of the surface, and film amplitudes depend on the boundary conditions of both surfaces. Combining Eqs. (A9), (A8), and (A5), we arrive at

$$\mathcal{G}_{\rm II}=B^2(\xi_0^+)^{d-2+\eta}\left(1+\epsilon\frac{n+2}{n+8}+O(\epsilon^2)\right)$$

$$\times R\frac{1}{\sqrt{\pi}}\frac{\Gamma(1/2-\eta/2)}{\Gamma(1-\eta/2)}. \quad \text{(A10)}$$

With $R\simeq 3.09$ [Eq. (A5)] and $\eta\simeq 0.031$ one has, for the three dimensional Ising model,

$$\mathcal{G}_{\rm II}=\mathcal{R}B^2(\xi_0^+)^{d-2+\eta}\simeq 4.21B^2(\xi_0^+)^{d-2+\eta}. \quad \text{(A11)}$$

APPENDIX B: ONE-LOOP RESULTS

1. Correlation functions for $z_1=z_2$

With the abbreviation $\tilde{\epsilon}=\epsilon[(n+2)/(n+8)]$, so that $\tilde{\epsilon}=\frac{1}{3}$, $\frac{2}{5}$, and $\frac{5}{11}$ for the Ising, *XY*, Heisenberg model in $d=3$, the renormalized two-point correlation function in one-loop order [Eqs. (2.3)–(2.6)] is given explicitly as (see also Ref. 84)

$$G(p,z,L=\infty,t=0)$$
$$=\mathcal{G}_{\rm II}z^{1-\eta}g_1(u=pz)$$
$$=\mu^{-\eta}z^{1-\eta}\left(\frac{1-e^{-2u}}{2u}+\frac{\tilde{\epsilon}}{4u}[-2Ei(-2u)\right.$$
$$\left.+e^{2u}Ei(-2u)+e^{-2u}Ei(2u)]+O(\epsilon^2)\right). \quad \text{(B1)}$$

$Ei(x)$ is the exponential integral function. In accordance with the normalization $g_1(0)=1$ this yields $\mathcal{G}_{\rm II}=\mu^{-\eta}[1+\tilde{\epsilon}+O(\epsilon^2)]$.

The temperature dependence is described by the scaling function $g_2(v)$, with $g_2(0)=1$:

$$G(p=0,z,L=\infty,t)=\mathcal{G}_{\rm II}z^{1-\eta}g_2(v=z/\xi)$$
$$=\mu^{-\eta}z^{1-\eta}\left[\frac{1-e^{-2v}}{2v}+\frac{\tilde{\epsilon}}{2v}\left((e^{-2v}-1)K_0(2v)+2e^{-2v}\sum_{k=0}^{\infty}v^{2k+1}\frac{\Psi(k+1)-\ln v+\frac{1}{2k+1}}{(k!)^2(2k+1)}\right)+O(\epsilon^2)\right]. \quad \text{(B2)}$$

$\Psi(x)$ and $K_0(x)$ denote the psi and Bessel functions, respectively[85] (see also Ref. 86).

Finally, the dependence of the critical structure factor on the film thickness is governed by a third scaling function $g_3(w)$, $g_3(0)=1$, $0\leq w\leq 1$:

$$G(p=0,z,L,t=0)=\mathcal{G}_{\rm II}z^{1-\eta}g_3(w=z/L)$$
$$=\mu^{-\eta}z^{1-\eta}\left[1-w+\tilde{\epsilon}\left\{-\frac{\pi^2}{18}w(1-w)^2-(1-2w)\left(1+C_E+\ln w+\frac{S_{3,2}^-(w)+I_2^-(w)}{w}\right)\right.\right.$$
$$\left.\left.+(1-w)[2+C_E+\ln w-S_{2,1}^+(w)-I_1^+(w)]\right\}+O(\epsilon^2)\right] \quad \text{(B3)}$$

with the abbreviations

$$S_{k,l}^{\pm}(w)=\sum_{n=k}^{\infty}\frac{B_n(-w)\pm B_n(w)}{n!(n-l)},$$

$$I_k^{\pm}(w)=\int_1^{\infty}\frac{dx}{e^x-1}\frac{e^{-xw}\pm e^{xw}}{x^k}. \quad \text{(B4)}$$

$B_n(w)$ are Bernoulli polynomials.[85] For the critical structure factor in the semi-infinite system, one has

$$G(p=0,z,L=\infty,t=0)=\mathcal{G}_{\rm II}z^{1-\eta}=\mu^{-\eta}z^{1-\eta}[1+\tilde{\epsilon}+O(\epsilon^2)]. \quad \text{(B5)}$$

From the explicit forms for g_i, $i=1$, 2, and 3, in Eqs. (B1) – (B3), together with $\eta_{\|}=2-\tilde{\epsilon}+O(\epsilon^2)$, one infers the limiting behaviors

$$g_1(u\to 0)=1+A_1u^{-1+\eta_{\|}}+O(u^2)$$

$$A_1=-[1+\tilde{\epsilon}(1-C_E-\ln 2)+O(\epsilon^2)], \quad \text{(B6)}$$

$$g_2(v\to 0)=1+B_1v^{-1+\eta_{\|}}+O(v^{1/\nu})$$

$$B_1=-[1+\tilde{\epsilon}(1-C_E)+O(\epsilon^2)], \quad \text{(B7)}$$

and

$$g_3(w\to 0)=1+C_1w^{-1+\eta_{\|}}+O(w^2)$$

$$C_1=-\left[1+\tilde{\epsilon}\left(\frac{\pi^2}{18}-C_E+2(S_2+I_1)-1\right)+O(\epsilon^2)\right], \quad \text{(B8)}$$

where $C_E\approx 0.5772$ is Euler's constant. S_2 is given by a sum over Bernoulli numbers and I_1 by integrals

$$S_2=\sum_{n=2}^{\infty}\frac{B_n}{n!(n-1)}\simeq 8.2877\times 10^{-2},$$

$$I_1=\int_1^{\infty}dx\,\frac{1}{e^x-1}\,\frac{1}{x}\simeq 0.2868. \tag{B9}$$

For the exponentiation of the scaling functions $h_1(u,v)$, $h_2(u,w)$, and $h_3(v,w)$, we have calculated the amplitude functions $H_1^{(1)}(\varphi)$, $H_1^{(2)}(\varphi)$, and $H_1^{(3)}(\varphi)$ [see Eqs. (3.14) and (3.15)]. Their ϵ expansions are

$$H_1^{(1)}(\varphi)=-\left[1-\tilde{\epsilon}\left(\ln\frac{\sin\varphi}{2}+\frac{\cos\varphi}{2}\ln\frac{1+\cos\varphi}{1-\cos\varphi}+a_1\right)+O(\epsilon^2)\right],$$

$$\varphi=\arctan[(p\xi)^{-1}], \tag{B10}$$

$$H_1^{(2)}(\varphi)=\sin(\varphi)\frac{1+e^{2\tan\varphi}}{1-e^{2\tan\varphi}}+\tilde{\epsilon}\left[\sin(\varphi)\frac{1+e^{2\tan\varphi}}{1-e^{2\tan\varphi}}\left(1-C_E-\ln(2\sin\varphi)-\mathcal{I}_0(\varphi)+\mathcal{I}_1(\varphi)\cot\varphi+\frac{1}{12}\cot^2\varphi\right)-\frac{\cos\varphi}{3(1-e^{2\tan\varphi})(1-e^{-2\tan\varphi})}\right]+O(\epsilon^2),$$

$$\varphi=\arctan(pL), \tag{B11}$$

and

$$H_1^{(3)}(\varphi)=\sin(\varphi)\frac{1+e^{2\tan\varphi}}{1-e^{2\tan\varphi}}+\tilde{\epsilon}\left(\sin(\varphi)\frac{1+e^{2\tan\varphi}}{1-e^{2\tan\varphi}}\times[1-C_E-\ln(\sin\varphi)+\mathcal{I}_1^{+}(\varphi)+\mathcal{I}_1^{-}(\varphi)]+\frac{\sin\varphi}{(1-e^{2\tan\varphi})(1-e^{-2\tan\varphi})}\times(2\pi+8\mathcal{I}_0^{0}(\varphi)\tan\varphi)\right)+O(\epsilon^2),$$

$$\varphi=\arctan(L/\xi), \tag{B12}$$

with $a_1\simeq 0.2704$ and the integrals

$$\mathcal{I}_0(\varphi)=\int_0^{\infty}\frac{dt}{e^t-1}\left(\frac{1}{t+2\tan\varphi}+\frac{1}{t-2\tan\varphi}\right), \tag{B13}$$

$$\mathcal{I}_1(\varphi)=\int_0^{\infty}\frac{dt}{e^t-1}\left(\frac{t}{t-2\tan\varphi}-\frac{t}{t+2\tan\varphi}\right), \tag{B14}$$

$$\mathcal{I}_0^{0}(\varphi)=\int_1^{\infty}dt\,\frac{\sqrt{t^2-1}}{e^{2t\tan\varphi}-1}, \tag{B15}$$

and

$$\mathcal{I}_1^{\pm}(\varphi)=\int_1^{\infty}dt\frac{\sqrt{t^2-1}}{e^{2t\tan\varphi}-1}\,\frac{t}{t\pm 1}. \tag{B16}$$

2. Correlation function for $z_1\neq z_2$

This is the most general case from which all results given above can be derived. We present $G(p,z_1,z_2,L,t)$ in terms of the scaling function g_{I} [Eq. (2.7)]:

$$G(p,z_1,z_2,L,t)=\mathcal{G}_{\mathrm{I}}p^{-1+\eta}g_{\mathrm{I}}(x=p\xi,u=z_1/\xi,v=z_2/\xi,y=L/\xi)$$
$$=\mu^{-\eta}p^{-1+\eta}\left[\frac{x}{2a}\left\{e^{-a|u-v|}-e^{-a(u+v)}+\frac{e^{-a(u-v)}+e^{-a(v-u)}-e^{-a(u+v)}-e^{a(u+v)}}{e^{2ya}-1}\right\}+\tilde{\epsilon}[\mathcal{J}_0(x,u,v,y)+\mathcal{J}_{\pi}(x,u,v,y)+\mathcal{J}_1(x,u,v,y)]+O(\epsilon^2)\right], \tag{B17}$$

with

$$\mathcal{J}_0(x,u,v,y)=-\frac{x}{a^3}\int_1^{\infty}ds\frac{\sqrt{s^2-1}}{e^{2ys}-1}\left\{e^{-a|u-v|}(1+a|u-v|)-e^{-a(u+v)}[1+a(u+v)]+\frac{1}{e^{2ya}-1}\left[e^{-a(u-v)}\left(1+a(u-v)+\frac{2ya}{1-e^{-2ya}}\right)+e^{-a(v-u)}\left(1+a(v-u)+\frac{2ya}{1-e^{-2ya}}\right)-e^{-a(u+v)}\left(1+a(u+v)+\frac{2ya}{1-e^{-2ya}}\right)-e^{a(u+v)}\left(1-a(u+v)+\frac{2ya}{1-e^{-2ya}}\right)\right]\right\}, \tag{B18}$$

$$\mathcal{J}_{\pi}(x,u,v,y)=\frac{\pi}{4}\frac{x}{a^2}\frac{1}{(1-e^{-2ya})^2}\{(1+e^{-2ya})(e^{-a(u+v)}+e^{a(u+v-2y)})-2e^{-2ya}(e^{-a(v-u)}+e^{-a(u-v)})\}, \tag{B19}$$

and

$$\mathcal{J}_1(x,u,v,y)=-\frac{1}{4}\frac{x}{a^2}\left\{e^{-a(u+v)}\frac{J(u,v)}{1-e^{-2ya}}+e^{a(u+v-2y)}\frac{J(y-u,y-v)}{1-e^{-2ya}}\right.$$
$$\left.-e^{-a(v-u)}\left(\Theta(v-u)+\frac{1}{e^{2ya}-1}\right)J(y-u,v)-e^{-a(u-v)}\left(\Theta(u-v)+\frac{1}{e^{2ya}-1}\right)J(y-v,u)\right\}, \quad \text{(B20)}$$

with $a=\sqrt{1+x^2}$ and

$$J(x_1,x_2)=\int_1^\infty ds\frac{\sqrt{s^2-1}}{1-e^{-2ys}}\left[\left(\frac{1}{s+a}-\frac{1}{s}\right)(e^{-2x_1s}+e^{-2x_2s})-\left(\frac{1}{s-a}-\frac{1}{s}\right)(e^{-2(y-x_1)s}+e^{-2(y-x_2)s})\right]. \quad \text{(B21)}$$

3. Susceptibility

The one-loop result of the total susceptibility [Eq. (3.23)] for Dirichlet boundary conditions is given by ($\gamma_s=\gamma+\nu$)

$$\chi(L,t)=B^2(\xi_0^+)^{d+1}\mathcal{R}\left(\frac{L}{\xi_0^+}\right)^{\gamma_s/\nu}f(y=L/\xi), \quad \text{(B22)}$$

with

$$f(y)=y^{-2}\left(1-\tilde{\epsilon}-\frac{2}{y}\left\{1+\tilde{\epsilon}\left[\pi\left(\frac{1}{2}-\frac{1}{\sqrt{3}}\right)-1\right]\right\}+\frac{4}{y}\frac{1}{e^y+1}-\tilde{\epsilon}\left\{\frac{4}{y}\frac{1}{e^y+1}+\frac{2}{y}\frac{e^{-y}}{(1+e^{-y})^2}\pi\left(1-\frac{1+e^{-y}}{\sqrt{3}}\right)\right.\right.$$
$$+\left(4+8\frac{e^{-y}}{(1+e^{-y})^2}-\frac{12}{y}\frac{1-e^{-y}}{1+e^{-y}}\right)\int_1^\infty ds\frac{\sqrt{s^2-1}}{e^{2sy}-1}+\frac{2}{y}\frac{1-e^{-y}}{1+e^{-y}}\int_1^\infty ds\frac{\sqrt{s^2-1}}{e^{2sy}-1}$$
$$\left.\left.\times\left(\frac{1}{s-1}-\frac{1}{s+1}+\frac{2}{s+1/2}-\frac{2}{s-1/2}\right)\right\}\right)+O(\epsilon^2). \quad \text{(B23)}$$

In the limit $y\to\infty$, the two integrals entering into Eq. (B23) vanish, $\sim e^{-2y}$, and therefore they do not contribute to the terms considered in Eq. (3.26). However, in the limit $y\to 0$ these two integrals contribute to the terms considered in Eq. (3.40):

$$J_0(y)=\int_1^\infty ds\frac{\sqrt{s^2-1}}{e^{2sy}-1}$$
$$=\frac{\pi^2}{24}y^{-2}-\frac{\pi}{4}y^{-1}+a_2-\frac{1}{4}\ln y+O(y) \quad \text{(B24)}$$

and

$$J_1(y)=\int_1^\infty ds\frac{\sqrt{s^2-1}}{e^{2sy}-1}\left(\frac{1}{s-1}-\frac{1}{s+1}+\frac{2}{s+1/2}-\frac{2}{s-1/2}\right)$$
$$=\pi\left(\sqrt{3}-\frac{3}{2}\right)y^{-1}-\frac{\pi}{2\sqrt{3}}+\frac{\sqrt{3}}{12}\pi y+b_2y^2-\frac{\sqrt{3}}{720}\pi y^3$$
$$+b_4y^4+O(y^5), \quad \text{(B25)}$$

with

$$a_2=\frac{5}{8}-\frac{1}{2}\left(\sum_{n=2}^\infty\frac{B_n}{n!(n-1)}+\int_1^\infty\frac{dx}{e^x-1}\frac{1}{x}\right)\simeq 0.440\,165, \quad \text{(B26)}$$

$$b_2=6\left(\sum_{n=0}^\infty\frac{B_n}{n!(n-3)}+\int_1^\infty\frac{dx}{e^x-1}\frac{1}{x^3}\right)$$
$$\simeq -9.131\,45\times 10^{-2},$$

$$b_4=18\left(\sum_{n=0}^\infty\frac{B_n}{n!(n-5)}+\int_1^\infty\frac{dx}{e^x-1}\frac{1}{x^5}\right)\simeq 5.9879\times 10^{-3}.$$

APPENDIX C: CROSS SECTION

1. Integration of the asymptotic limits

Equation (4.10) involves integrals of the following kind:

$$\int_0^L dz_1e^{-\kappa_1z_1}\int_0^L dz_2e^{-\kappa_2z_2}G(p,z_1,z_2,L,t), \quad \text{(C1)}$$

where $\kappa_j\in\{\pm i[q_2(\alpha_f)\pm q_2(\alpha_i)],\ \pm i[q_2^*(\alpha_f)\pm q_2^*(\alpha_i)]\}$, $j=1$ and 2 [see Eq. (4.2), as well as Eqs. (D1) and (D2) in Appendix D] and $\kappa_j(\alpha)\equiv Kf_j(\alpha_i,\alpha_f,\alpha_{c12})$ (see above). The asymptotic behavior of Eqs. (3.19), (3.20), and (3.21) can be summarized by the formula

$$G_{as}(p,z_1,z_2,L,t)=\mathcal{G}_{\rm II}\Bigg\{\Theta(z_2-z_1)z_1^{1-\eta}\left(\frac{z_2}{z_1}\right)^{1-\eta_\perp}+\Theta(z_1-z_2)z_2^{1-\eta}\left(\frac{z_1}{z_2}\right)^{1-\eta_\perp}+\mathcal{C}\Bigg(\Theta(z_2-z_1)z_1^{1-\eta}\left(\frac{z_2}{z_1}\right)^{1-\eta_\perp}z_2^{-1+\eta_\parallel}+\Theta(z_1-z_2)z_2^{1-\eta}\left(\frac{z_1}{z_2}\right)^{1-\eta_\perp}z_1^{-1+\eta_\parallel}\Bigg)\Bigg\}$$
$$=\mathcal{G}_{\rm II}\{d(z_1,z_2)+a(p,z_1,z_2,L,t)\}. \quad \text{(C2)}$$

The expression $d(z_1,z_2)$ corresponds to the leading contribution $\mathcal{C}=0$. $\mathcal{C}$ is an abbreviation for the three quantities $A_1p^{-1+\eta_\parallel}$ for $t=0$ and $L=\infty$, $B_1(1/\xi)^{-1+\eta_\parallel}$ for $p=0$ and $L=\infty$, and $C_1(1/L)^{-1+\eta_\parallel}$ for $p=t=0$ in Eqs. (3.19), (3.20), and (3.21). For the quasi-Laplace transform of the contribution $d(z_1,z_2)$,

$$\overline{\mathcal{D}}(\kappa_1,\kappa_2,L)=\int_0^L dz_1e^{-\kappa_1z_1}\int_0^L dz_2e^{-\kappa_2z_2}d(z_1,z_2) \quad \text{(C3)}$$

one finds, with $f_j=\kappa_j/K$, $j=1$ and 2,

$$\overline{\mathcal{D}}(\kappa_1,\kappa_2,L)\equiv\overline{\mathcal{D}}(f_1,f_2,LK)=K^{-3+\eta}\Bigg[\frac{1}{f_1f_2(f_1+f_2)}-\frac{e^{-f_1LK}}{f_2^2f_1}-\frac{e^{-f_2LK}}{f_1^2f_2}+e^{-(f_1+f_2)LK}\left(\frac{LK}{f_1f_2}+\frac{f_1^2+f_1f_2+f_2^2}{f_1^2f_2^2(f_1+f_2)}\right)$$
$$+\frac{\tilde{\epsilon}}{2}\Bigg\{\frac{-2}{f_1f_2(f_1+f_2)}-e^{-(f_1+f_2)LK}\frac{f_1^2+f_2^2}{f_1^2f_2^2(f_1+f_2)}+\frac{1}{f_1^2f_2}[\ln(f_1/f_2+1)+Ei(1,(f_1+f_2)LK)-Ei(1,f_2LK)]$$
$$+\frac{1}{f_2^2f_1}[\ln(f_2/f_1+1)+Ei(1,(f_1+f_2)LK)-Ei(1,f_1LK)]+\frac{e^{-f_1LK}}{f_2^2f_1}[1-C_E-\ln f_2-\ln LK-Ei(1,f_2LK)]$$
$$+\frac{e^{-f_2LK}}{f_1^2f_2}[1-C_E-\ln f_1-\ln LK-Ei(1,f_1LK)]\Bigg\}+O(\epsilon^2)\Bigg]. \quad \text{(C4)}$$

In the limiting case of a semi-infinite film ($L\to\infty$), Eq. (C4) reduces to

$$\overline{\mathcal{D}}(f_1,f_2,LK=\infty)=K^{-3+\eta}\left[\frac{1}{f_1f_2(f_1+f_2)}\left(1+\tilde{\epsilon}\left\{1-\frac{f_1+f_2}{2f_1}\ln(1+f_1/f_2)-\frac{f_1+f_2}{2f_2}\ln(1+f_2/f_1)\right\}\right)+O(\epsilon^2)\right]. \quad \text{(C5)}$$

The corresponding expression for the leading correction term

$$\overline{\mathcal{A}}(f_1,f_2,LK)=\int_0^L dz_1e^{-\kappa_1z_1}\int_0^L dz_2e^{-\kappa_2z_2}a(p,z_1,z_2,L,t) \quad \text{(C6)}$$

is

$$\overline{\mathcal{A}}(f_1,f_2,LK)=K^{-3+\eta}K^{1-\eta_\parallel}\mathcal{C}\Bigg[\frac{1}{f_1^2f_2^2}\{1-e^{-f_1LK}(1+f_1LK)-e^{-f_2LK}(1+f_2LK)$$
$$+e^{-(f_1+f_2)LK}[1+(f_1+f_2)LK+f_1f_2(LK)^2]\}$$
$$-\frac{\tilde{\epsilon}}{2}\frac{1}{f_1^2f_2^2}(2-2C_E-\ln f_1f_2-Ei(1,f_1LK)-Ei(1,f_2LK)$$
$$+e^{-f_1LK}\{-1+(1+f_1LK)[C_E-1+\ln f_2-\ln LK+Ei(1,f_2LK)]\}$$
$$+e^{-f_2LK}\{-1+(1+f_2LK)[C_E-1+\ln f_1-\ln LK+Ei(1,f_1LK)]\}$$
$$+e^{-(f_1+f_2)LK}[LK(f_1+f_2)(1+2\ln LK)+2(1+\ln LK)+2f_1f_2(LK)^2\ln LK])+O(\epsilon^2)\Bigg], \quad \text{(C7)}$$

with the semi-infinite limit $L\to\infty$:

$$\overline{\mathcal{A}}(f_1,f_2,LK=\infty)=K^{-3+\eta}K^{1-\eta_\parallel}\mathcal{C}'\left[\frac{1}{f_1^2f_2^2}\left(1+\tilde{\epsilon}\left\{C_E-1+\frac{1}{2}\ln f_1f_2\right\}\right)+O(\epsilon^2)\right], \quad \text{(C8)}$$

where $\mathcal{C}'$ is an abbreviation for the two quantities $A_1 p^{-1+\eta_\parallel}$, for $t=0$ and $L=\infty$, and $B_1(1/\xi)^{-1+\eta_\parallel}$, for $p=0$ and $L=\infty$. Distant wall corrections to the semi-infinite system vanish exponentially. In order to obtain the analytic expressions in Eqs. (C4) and (C7), we have expanded $d(z_1,z_2)$ and $a(p,z_1,z_2,L,t)$ in terms of ϵ using for the ϵ expansion of the exponents $\eta_\parallel=2-\tilde{\epsilon}+O(\epsilon^2)$, $\eta_\perp=1-\tilde{\epsilon}/2+O(\epsilon^2)$, and $\eta=O(\epsilon^2)$. The function $Ei(1,z)$ is the exponential integral defined by

$$Ei(1,z)=\int_1^\infty \frac{e^{-zt}}{t}dt=-Ei(-z). \tag{C9}$$

This function is numerically more suitable than the exponential integral $Ei(z)$,

$$Ei(z)=-\int_{-z}^{\infty}\frac{e^{-t}}{t}dt, \tag{C10}$$

appearing in the formulas for the correlation function.

2. Integration of the mean-field correlation function

Equation (C1) for the full mean-field correlation function yields

$$\begin{aligned}
&\mathcal{S}[b=\sqrt{(p/K)^2+(\xi K)^{-2}},LK,f_1,f_2]\\
&\quad=\int_0^L dz_1 e^{-\kappa_1 z_1}\int_0^L dz_2 e^{-\kappa_2 z_2}G(p,z_1,z_2,L,t)\\
&\quad=\mathcal{G}_{\mathrm{II}}K^{-3+\eta}\frac{1}{2b}\left\{\frac{1-e^{-(f_1+b)LK}}{(f_1+b)(f_2-b)}-\frac{1-e^{-(f_1+f_2)LK}}{(f_1+f_2)(f_2-b)}+\frac{1-e^{-(f_1+f_2)LK}}{(f_1+f_2)(f_2+b)}\right.\\
&\qquad-\frac{e^{-(f_2+b)LK}-e^{-(f_1+f_2)LK}}{(f_1-b)(f_2+b)}-\frac{(1-e^{-(f_1+b)LK})(1-e^{-(f_2+b)LK})}{(f_1+b)(f_2+b)}\\
&\qquad+\frac{1}{e^{2bLK}-1}\left(\frac{(1-e^{-(f_1+b)LK})(1-e^{-(f_2-b)LK})}{(f_1+b)(f_2-b)}+\frac{(1-e^{-(f_1-b)LK})(1-e^{-(f_2+b)LK})}{(f_1-b)(f_2+b)}\right.\\
&\qquad\left.\left.-\frac{(1-e^{-(f_1+b)LK})(1-e^{-(f_2+b)LK})}{(f_1+b)(f_2+b)}-\frac{(1-e^{-(f_1-b)LK})(1-e^{-(f_2-b)LK})}{(f_1-b)(f_2-b)}\right)\right\},
\end{aligned} \tag{C11}$$

using the notation of Appendix C 1. The above formula exhibits the following limiting expressions:

$$\mathcal{S}(b=0,LK=\infty,f_1,f_2)=\mathcal{G}_{\mathrm{II}}K^{-3+\eta}\frac{1}{(f_1+f_2)f_1f_2}, \tag{C12}$$

$$\mathcal{S}(b,LK=\infty,f_1,f_2)=\mathcal{G}_{\mathrm{II}}K^{-3+\eta}\frac{1}{(f_1+f_2)(f_1+b)(f_2+b)}, \tag{C13}$$

and

$$\begin{aligned}
\mathcal{S}(b=0,LK,f_1,f_2)&=\mathcal{G}_{\mathrm{II}}K^{-3+\eta}\left\{\frac{1}{(f_1+f_2)f_1f_2}-\frac{1}{f_1^2f_2^2}\frac{1}{LK}\right.\\
&\quad+\frac{e^{-f_1LK}+e^{-f_2LK}}{f_1^2f_2^2}\frac{1}{LK}\\
&\quad\left.-\left(\frac{1}{(f_1+f_2)f_1f_2}+\frac{1}{f_1^2f_2^2}\frac{1}{LK}\right)e^{-(f_1+f_2)LK}\right\}.
\end{aligned} \tag{C14}$$

Equations (C12)–(C14) lead to the following three cusp singularities:

$$\frac{\mathcal{S}(p\to 0,t=0,LK=\infty,f_1,f_2)}{\mathcal{S}(p=0,t=0,LK=\infty,f_1,f_2)}=1-\left[\frac{f_1+f_2}{f_1f_2}\right]^{-1+\eta_\parallel}\left(\frac{p}{K}\right)^{-1+\eta_\parallel}+O(p^2), \tag{C15}$$

$$\frac{\mathcal{S}(p=0,t\to 0,LK=\infty,f_1,f_2)}{\mathcal{S}(p=0,t=0,LK=\infty,f_1,f_2)}=1-\left[\frac{f_1+f_2}{f_1f_2}\right]^{-1+\eta_\parallel}\times\left(\frac{1}{\xi K}\right)^{-1+\eta_\parallel}+O(\xi^{1/\nu}), \tag{C16}$$

and

$$\frac{\mathcal{S}(p=0,t=0,LK\to\infty,\tilde f_1,\tilde f_2)}{\mathcal{S}(p=0,t=0,LK=\infty,f_1,f_2)}=\frac{f_1f_2(f_1+f_2)}{\tilde f_1\tilde f_2(\tilde f_1+\tilde f_2)}-\left[\frac{f_1f_2(f_1+f_2)}{\tilde f_1^2\tilde f_2^2}\right]^{-1+\eta_\parallel}\times\left(\frac{1}{LK}\right)^{-1+\eta_\parallel}+O(e^{-L}). \tag{C17}$$

We note that the last two arguments of the nominator and denominator on the left-hand side of Eq. (C17) are in general, as indicated, different from each other. For $L=\infty$ the variables f_j are given by $-i[q_2(\alpha_f)+q_2(\alpha_i)]/K$ or $i[q_2^*(\alpha_i)+q_2^*(\alpha_f)]/K$, whereas for $L<\infty$ the variables $\tilde f_j$ are given by $-i[kq_2(\alpha_f)+lq_2(\alpha_i)]/K$ or $i[mq_2^*(\alpha_i)+nq_2^*(\alpha_f)]/K$ with any combination of $k,l,m,n=\pm 1$ [see the exponentials in the last lines of Eqs. (D1) and (D2) in Appendix D].

For the exponentiation of the p-L, ξ-L, and p-ξ dependences, we introduce polar coordinates [see Eq. (3.13)]

$$\omega=\sqrt{(p/K)^2+(LK)^{-2}},\quad \varphi=\arctan(pL),\qquad \frac{1}{LK}=\omega\cos\varphi,\quad \frac{p}{K}=\omega\sin\varphi \tag{C18}$$

leading to the scaling function $\mathcal{S}(\omega,\varphi,\tilde f_1,\tilde f_2)=\mathcal{S}(p/K=\omega\sin\varphi, LK=(\omega\cos\varphi)^{-1},\tilde f_1,\tilde f_2)$ and to its asymptotic expansion

$$\frac{\mathcal{S}(\omega\to 0,\varphi,\tilde f_1,\tilde f_2)}{\mathcal{S}(\omega=0,f_1,f_2)}=\frac{f_1f_2(f_1+f_2)}{\tilde f_1\tilde f_2(\tilde f_1+\tilde f_2)}-\sin(\varphi)\,\frac{1+e^{-2\tan\varphi}}{1-e^{-2\tan\varphi}}\times\left[\frac{f_1f_2(f_1+f_2)}{\tilde f_1^2\tilde f_2^2}\right]^{-1+\eta_\parallel}\omega^{-1+\eta_\parallel}+\cdots. \tag{C19}$$

Because in this section we consider only mean-field scaling functions, a simple substitution of the scaling variable p/K by $1/\xi K$ in Eq. (C18) leads to the same result for the ξ-L dependences. The semi-infinite system is described by the coordinates

$$\omega=\sqrt{(p/K)^2+(\xi K)^{-2}},\qquad \varphi=\arctan\frac{1}{p\xi},\qquad \frac{1}{\xi K}=\omega\sin\varphi,\quad \frac{p}{K}=\omega\cos\varphi, \tag{C20}$$

leading to the asymptotic behavior of the scaling function

$$\frac{\mathcal{S}(\omega\to 0,f_1,f_2)}{\mathcal{S}(\omega=0,f_1,f_2)}=1-\left[\frac{f_1+f_2}{f_1f_2}\right]^{-1+\eta_\parallel}\omega^{-1+\eta_\parallel}+\cdots, \tag{C21}$$

which is independent of φ.

APPENDIX D: PRODUCTS OF WAVE FUNCTIONS

In order to illustrate the type of transformations appearing in Eqs. (4.10) and (C1), we present the explicit expression for the product of wave functions in Eq. (4.2):

$$\begin{aligned}\psi_f(z_1)\psi_i(z_1)\psi_i^*(z_2)\psi_f^*(z_2)&=[s_+(\alpha_f)e^{iq_2(\alpha_f)z_1}+s_-(\alpha_f)e^{-iq_2(\alpha_f)z_1}][s_+(\alpha_i)e^{iq_2(\alpha_i)z_1}+s_-(\alpha_i)e^{-iq_2(\alpha_i)z_1}]\\&\quad\times[s_+^*(\alpha_i)e^{-iq_2^*(\alpha_i)z_2}+s_-^*(\alpha_i)e^{iq_2^*(\alpha_i)z_2}][s_+^*(\alpha_f)e^{-iq_2^*(\alpha_f)z_2}+s_-^*(\alpha_f)e^{iq_2^*(\alpha_f)z_2}]\\&=\sum_{k,l,m,n=\pm}s_k(\alpha_f)s_l(\alpha_i)s_m^*(\alpha_i)s_n^*(\alpha_f)e^{i[kq_2(\alpha_f)+lq_2(\alpha_i)]z_1}e^{-i[mq_2^*(\alpha_i)+nq_2^*(\alpha_f)]z_2},\end{aligned} \tag{D1}$$

where s and q are defined in Eqs. (4.3) and (4.4). Thus the scattering cross section is proportional to a sum of 16 terms involving integrations over z_1 and z_2.

For the limiting case of a semi-infinite half-space one has

$$\begin{aligned}\psi_{\infty/2}^f(z_1)\psi_{\infty/2}^i(z_1)\psi_{\infty/2}^{(i)*}(z_2)\psi_{\infty/2}^{(f)*}(z_2)&=t_{si}(\alpha_f)e^{iq_2(\alpha_f)z_1}t_{si}(\alpha_i)e^{iq_2(\alpha_i)z_1}t_{si}^*(\alpha_i)e^{-iq_2^*(\alpha_i)z_2}t_{si}^*(\alpha_f)e^{-iq_2^*(\alpha_f)z_2}\\&=|t_{si}(\alpha_f)|^2|t_{si}(\alpha_i)|^2e^{i[q_2(\alpha_f)+q_2(\alpha_i)]z_1}e^{-i[q_2^*(\alpha_i)+q_2^*(\alpha_f)]z_2}.\end{aligned} \tag{D2}$$

In this limit the above sum reduces to a single term.

[1] M. A. Herman and H. Sitter, *Molecular Beam Epitaxy*, Springer Series in Materials Science Vol. 7 (Springer, Heidelberg, 1996).
[2] S. Dietrich, in *Phase Transitions and Critical Phenomena*, edited by C. Domb and J. L. Lebowitz (Academic, New York, 1988), Vol. 12, p. 1.
[3] R. Evans. J. Phys.: Condens. Matter **2**, 8989 (1990).
[4] J.A. Duffy, N.J. Wilkinson, H.M. Fretwell, M.A. Alam, and R. Evans, J. Phys.: Condens. Matter **7**, L713 (1995); D.W. Brown, P.E. Sokol, and S.N. Ehrlich, Phys. Rev. Lett. **81**, 1019 (1998).
[5] A.H. Marcus and S.A. Rice, Phys. Rev. Lett. **77**, 2577 (1996); Phys. Rev. E **55**, 637 (1997).
[6] G. An and M. Schick, J. Phys. A: Math. Gen. **21**, L213 (1988).
[7] M. E. Fisher, in *Critical Phenomena*, Proceedings of the 1970 International School of Physics ''Enrico Fermi,'' Course LI, edited by M. S. Green (Academic, New York, 1971), p. 1.
[8] M.I. Kaganov and A.N. Omel'Yanchuk, Zh. Éksp. Teor. Fiz. **61** 1679 (1971) [Sov. Phys. JETP **34**, 895 (1972)].
[9] M. Nauenberg, J. Phys. A: Math. Gen. **8**, 925 (1975).
[10] M. Suzuki, Prog. Theor. Phys. **58**, 1142 (1977).
[11] A.N. Berker and S. Ostlund, J. Phys. C **12**, 4961 (1979).
[12] L.G. Dunfield and J. Noolandi, Phys. Rev. B **22**, 4430 (1980).
[13] E. Brézin, J. Phys. (Paris) **43**, 15 (1982).
[14] P. Nightingale, J. Appl. Phys. **53**, 7927 (1982).
[15] M. N. Barber, in *Phase Transitions and Critical Phenomena*, edited by C. Domb and J. L. Lebowitz (Academic, London, 1983), Vol. 8, p. 145.
[16] E. Brézin and J. Zinn-Justin, Nucl. Phys. B **257**, 867 (1985).
[17] J. Rudnick, H. Guo, and D. Jasnow, J. Stat. Phys. **41**, 353 (1985).
[18] K. Binder and P.C. Hohenberg, Phys. Rev. B **6**, 3461 (1972).
[19] M.E. Fisher and M.N. Barber, Phys. Rev. Lett. **28**, 1516 (1972).
[20] M.N. Barber, Phys. Rev. B **8**, 407 (1973).
[21] D.S. Ritchie and M.E. Fisher, Phys. Rev. B **7**, 480 (1973).
[22] T.W. Capehart and M.E. Fisher, Phys. Rev. B **13**, 5021 (1976).
[23] D.J.E. Callaway and M. Schick, Phys. Rev. B **23**, 3494 (1981).
[24] G. A. T. Allan, Phys. Rev. B **1**, 352 (1970).
[25] A.J. Bray and M.A. Moore, J. Phys. A: Math. Gen. **4**, 715 (1978).
[26] H. Nakanishi and M.E. Fisher, J. Chem. Phys. **78**, 3279 (1983).
[27] M.I. Kaganov, Zh. Éksp. Teor. Fiz. **62**, 1196 (1972) [Sov. Phys. JETP **35**, 631 (1972)].
[28] J. Rudnick and D. Jasnow, Phys. Rev. Lett. **49**, 1595 (1982).
[29] M. Krech and S. Dietrich, Phys. Rev. Lett. **66**, 345 (1991).
[30] (a) M. Krech and S. Dietrich, Phys. Rev. A **46**, 1886 (1992); (b) **46**, 1922 (1992).
[31] E. Eisenriegler, M. Krech, and S. Dietrich, Phys. Rev. Lett. **70**, 619 (1993).
[32] M. Krech, *The Casimir Effect in Critical Systems* (World Scientific, Singapore, 1994).
[33] P. Sutter and V. Dohm, Physica B **194**, 613 (1994).
[34] X.S. Chen, V. Dohm, and A. Esser, J. Phys. I **5**, 205 (1995).
[35] M. Krech, Phys. Rev. E **56**, 1642 (1996).
[36] D. Schmeltzer, Phys. Rev. B **32**, 7512 (1985).
[37] D. O'Connor and C.R. Stephens, Nucl. Phys. B **360**, 297 (1991); J. Phys. A: Math. Gen. **25**, 101 (1992); Phys. Rev. Lett. **72**, 506 (1994); Proc. R. Soc. London, Ser. A **444**, 287 (1994); F. Freire, D. O'Connor, and C.R. Stephens, J. Stat. Phys. **74**, 219 (1994).
[38] F. M. Gasparini and I. Rhee, in *Progress in Low Temperature Physics*, edited by D. F. Brewer (North-Holland, Amsterdam, 1992), Vol. XIII, p. 1.
[39] D. Lederman, C.A. Ramos, V. Jaccarino, and J.L. Cardy, Phys. Rev. B **48**, 8365 (1993).
[40] J.A. Nissen, T.C.P. Chui, and J.A. Lipa, J. Low Temp. Phys. **92**, 352 (1993).
[41] S. Mehta and F.M. Gasparini, Phys. Rev. Lett. **78**, 2596 (1997).
[42] S. Andrieu, M. Finazzi, Ph. Bauer, H. Fisher, P. Lefevre, A. Traverse, K. Hircovini, G. Krill, and M. Piecuch, Phys. Rev. B **57**, 1985 (1998).
[43] M. Henkel, S. Andrieu, Ph. Bauer, and M. Piecuch, Phys. Rev. Lett. **80**, 4783 (1998).
[44] K. Binder and D.P. Landau, Phys. Rev. B **37**, 1745 (1988).
[45] K. Binder, D.P. Landau, and A.M. Ferrenberg, Phys. Rev. Lett. **74**, 298 (1995).
[46] K. Binder, P. Nielba, and V. Pereyara, Z. Phys. B **104**, 81 (1997).
[47] K. Binder, in *Phase Transitions and Critical Phenomena*, edited by C. Domb and J. L. Lebowitz (Academic, London, 1983), Vol. 8, p. 1.
[48] H. W. Diehl, in *Phase Transitions and Critical Phenomena*, edited by C. Domb and J. L. Lebowitz (Academic, London, 1986), Vol. 10, p. 75.
[49] S. Dietrich and A. Haase, Phys. Rep. **260**, 1 (1995).
[50] H. Dosch, *Critical Phenomena at Surfaces and Interfaces: Evanescent X-Ray and Neutron Scattering*, Springer Tracts in Modern Physics Vol. 126 (Springer, Heidelberg, 1992).
[51] L. Mailänder, H. Dosch, J. Peisl, and R.L. Johnson, Phys. Rev. Lett. **64**, 2527 (1990).
[52] H. Dosch, L. Mailänder, R.L. Johnson, and J. Peisl, Surf. Sci. **279**, 367 (1992).
[53] H. Dosch, Int. J. Mod. Phys. B **6**, 2773 (1992).
[54] S. Krimmel, W. Donner, B. Nickel, H. Dosch, C. Sutter, and G. Grübel, Phys. Rev. Lett. **78**, 3880 (1997).
[55] S. Dietrich and H. Wagner, Phys. Rev. Lett. **51**, 1469 (1983).
[56] S. Dietrich and H. Wagner, Z. Phys. B **56**, 207 (1984).
[57] A. Drewitz, R. Leidl, T.W. Burkhardt, and H.W. Diehl, Phys. Rev. Lett. **78**, 1090 (1997).
[58] R. Leidl and H.W. Diehl, Phys. Rev. B **57**, 1908 (1998).
[59] E. Eisenriegler, M. Krech, and S. Dietrich, Phys. Rev. B **53**, 14 377 (1996).
[60] L. Guttmann, Solid State Phys. **56**, 146 (1956).
[61] L. Guttmann, H.C. Schnyders, and G.J. Arai, Phys. Rev. Lett. **22**, 517 (1969).
[62] L. Guttmann and H.C. Schnyders, Phys. Rev. Lett. **22**, 520 (1969).
[63] J.A. Oyedele and M.F. Collins, Phys. Rev. B **16**, 3208 (1977).
[64] J. Als-Nielsen and O.W. Dietrich, Phys. Rev. **153**, 706 (1967).
[65] H.W. Diehl, Int. J. Mod. Phys. B **11**, 3503 (1997).
[66] U. Ritschel and P. Czerner, Phys. Rev. Lett. **77**, 3645 (1996); U. Ritschel, Phys. Rev. B **57**, R693 (1998).
[67] H. Dosch, Physica B **192**, 163 (1993).
[68] A.M. Nemirovsky and K.F. Freed, Nucl. Phys. B **270**, 423 (1986).
[69] S. Allen and R.K. Pathria, Phys. Rev. B **50**, 6765 (1994).
[70] M. Krech, E. Eisenriegler, and S. Dietrich, Phys. Rev. E **52**, 1345 (1995).
[71] D. J. Amit, *Field Theory, the Renormalization Group, and Critical Phenomena* (McGraw-Hill, New York, 1978).
[72] H.B. Tarko and M.E. Fisher, Phys. Rev. B **11**, 1217 (1975).
[73] H.W. Diehl and S. Dietrich, Z. Phys. B **42**, 65 (1981).
[74] G. Gompper, Z. Phys. B **56**, 217 (1984).
[75] G. Gompper, Z. Phys. B **62**, 357 (1986).
[76] J.L. Cardy, Nucl. Phys. B **240**, 514 (1984).
[77] G. Gompper, Ph.D. thesis, University of Munich, 1986.

[78] A.O. Parry and P.S. Swain, J. Phys.: Condens. Matter **9**, 2351 (1997).
[79] C. Bervillier, Phys. Rev. B **14**, 4964 (1976).
[80] V. Privman, P.C. Hohenberg, and A. Aharony, in *Phase Transitions and Critical Phenomena*, edited by C. Domb and J. L. Lebowitz (Academic, London, 1991), Vol. 14, p. 1.
[81] H.W. Diehl, G. Gompper, and W. Speth, Phys. Rev. B **31**, 5841 (1985).
[82] M.M. Leite, M. Sardelich, and M.D. Coutinho-Filho, Phys. Rev. E **59**, 2683 (1999).
[83] S. Dietrich and H. Wagner, Z. Phys. B **59**, 35 (1985).
[84] H.W. Diehl and S. Dietrich, Z. Phys. B **50**, 117 (1983).
[85] I. S. Gradshteyn and I. M. Ryzhik, *Table of Integrals, Series, and Products* (Academic, New York, 1965).
[86] A.M. Nemirovsky, Zhen-Gang Wang, and K.F. Freed, Phys. Rev. B **36**, 3755 (1987).